NATIONAL ADVISORY COMMITTEE FOR AERONAUTICS

TECHNICAL NOTE 3733

PROBABILITY AND FREQUENCY CHARACTERISTICS OF SOME FLIGHT BUFFET LOADS

By Wilber B. Huston and T. H. Skopinski

Langley Aeronautical Laboratory
Langley Field, Va.

Washington
August 1956

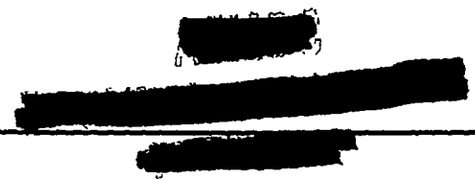

TABLE OF CONTENTS

NATIONAL ADVISORY COMMITTEE FOR AERONAUTICS

TECHNICAL NOTE 3733

PROBABILITY AND FREQUENCY CHARACTERISTICS OF SOME FLIGHT BUFFET LOADS

By Wilber B. Huston and T. H. Skopinski

SUMMARY

The frequency characteristics and statistical properties of the buffet loads measured on the unswept wing and tail of a fighter airplane have been studied in the stall and in the shock regime. The results indicate that the wing loads in buffeting can be treated as the Gaussian response of a simple elastic system. The tail loads appear to represent a more complicated process.

INTRODUCTION

The fluctuating loads imposed on an aircraft structure in the stalled flight condition have been studied extensively since their potentially destructive character was revealed in 1930 (ref. 1). Although first interest was centered on "tail buffeting," in which loads are induced on the tail by flow disturbances in the wake which have their origin in the separated flow over the stalled wing, it was soon realized that this induced or secondary buffeting was only part of a larger class of separation phenomena and that the separated flow over the wing could also produce appreciable loads in the airplane structure. The term "buffeting" is now generally used to include this primary buffeting as well as the secondary or induced type. As the speed of airplanes has been extended into the transonic and supersonic ranges, the term buffeting has also been applied when the separation is associated with shock formation or other complex flow patterns in the higher speed ranges. Buffeting is also used to characterize both the aerodynamic excitation and the resultant structural loads.

In attempts at quantitative treatment of buffet loads, a major difficulty is found in the random character of the fluctuations, which has led to uncertainty in the application of any simple numerical measure (such as the frequently used half of the peak-to-peak value). This randomness has been recognized by many workers, but the possible applicability of the analytical and experimental tools developed in the study of random processes was first pointed out in 1951 (ref. 2). Some experimental

evidence for this applicability was provided by the analysis of reference 3, where the peak values of wing and tail root structural shear measured in stalls of varying duration at various speeds and altitudes were found to correlate well with certain parameters suggested by consideration of the linear response of an aerodynamically damped elastic system to an aerodynamic excitation which is a Gaussian random process.

The Gaussian random process, which is discussed in more detail in the body of the paper and in appendix A, is a special type of random process about which much more is known than any other type (refs. 4 to 7). Of particular interest is the fact that the statistical properties of such a process are simply related to its frequency characteristics as represented by the power spectrum. A primary purpose of the present study, therefore, is to examine the character of the wing and tail loads in buffeting in order to determine how well buffet loads approximate a Gaussian random process. For this purpose a number of characteristics of the load time histories are evaluated and compared with what would be expected for a Gaussian process. In addition to the power spectrum, the characteristics examined are the probability distribution of the loads, the frequency of zero crossings, and the probability distribution of the peak loads. These properties were chosen because they could be readily evaluated and are of interest in connection with the study of fatigue.

Inasmuch as buffeting was encountered during maneuvering flight, the time histories of measured wing and tail loads contained large-amplitude components at low frequencies in addition to the more rapid load fluctuations of buffeting. A brief account of the numerical methods utilized for the study of buffeting under these conditions is included.

SYMBOLS

C_N	airplane normal-force coefficient
f	frequency, cps
f_F	folding frequency, $\frac{1}{2\,\Delta t}$, cps
f_0	average number of crossings per second of the zero axis with positive (or negative) slope
f_p	average number of positive (or negative) peaks per second
k_1, k_2	constants of the peak probability distribution (defined in eqs. (9) and (10))

L buffet component of root structural shear load, lb

ΔL largest value of L in a specified time interval, lb

M Mach number

N number in sample

N_L average number of peaks per second which exceed a given value of L

$P(y)$ probability that a value of the random variable y will be exceeded

P penetration (beyond the buffet boundary), $\frac{C_N - C_{N_{BB}}}{C_{N_{max}} - C_{N_{BB}}}$

q dynamic pressure, lb/sq ft

t time, sec

T a specified time interval, sec

y a random variable

z standard variable, $\frac{y - \bar{y}}{\sigma}$

α angle of attack, deg

σ standard deviation

$\Phi(f)$ power spectral density function of buffet load, lb^2/cps

$\lfloor \ \rfloor$ row matrix

$\{ \}$ column matrix

$\| \ \|$ rectangular matrix

Subscripts:

BB buffet boundary

N relating to normal probability functions

P relating to peak probability functions

t tail

w wing

max maximum

Time differentiation is denoted by dots (as $\dot{y}$, $\ddot{y}$, etc.)

SCOPE AND GENERAL CHARACTERISTICS OF FLIGHT BUFFET-LOAD DATA

The flight data analyzed in the present investigation were acquired in the course of the flight investigation of the wing and tail buffet loads reported in reference 3. The airplane, flight instrumentation, and data-reduction procedures are described in reference 3. Some characteristic structural vibration frequencies of the airplane are listed in table I. The present study, which deals with time histories of the wing and tail root structural shear, required a more detailed evaluation of the strain-gage records than was required for reference 3, which deals with maximum values (one-half of the largest peak-to-peak fluctuation) encountered in a run. The measured root structural shear in buffeting was composed of two components: a maneuvering load (slow variations over a range of 20,000 pounds in the case of the wing) and a superimposed buffet load (comparatively rapid fluctuations of as much as ±3,900 pounds). For study of the statistical properties of the buffet loads, separation of the buffet component from the measured values of load was required. This separation was accomplished by means of a numerical filtering technique which, since it may be of use in the study of other flight buffet measurements, is described in appendix B.

Maneuvers Investigated

Of the 194 runs reported in reference 3, six were selected for the detailed evaluation required in the present investigation, three in the stall regime and three in the shock regime. Four runs were obtained with the basic airplane and two with the modified airplane, that is, the airplane with 100-pound weights added internally near the wing tips in order to lower the natural frequency of the wing in the fundamental bending mode from 11.7 to 9.3 cps. The results for two of the six runs are reported herein, since they were found to be typical. Run A is a gradual pull-up to the stall with the modified airplane at a Mach number of 0.46; run B, with the basic configuration, is a gradual pull-up into the buffet region at a Mach number of 0.74. The variation of airplane normal-force coefficient and Mach number in relation to the buffet boundary of the airplane is shown for these runs in figure 1. The arrows in figure 1 represent flight conditions for the onset and end of buffeting as evidenced by the accelerometer at the center of gravity.

Time History of Flight Condition and Buffet Intensity

The time variations of airplane normal-force coefficient, Mach number, and buffet intensity for runs A and B are shown in figure 2. Angle-of-attack values are also given for run A. The measure of buffet intensity, denoted by the symbol $\sigma(t)$, is the root-mean-square value of the buffeting shear in a 1/2-second period; that is,

$$\sigma(t)=\left[\frac{1}{T}\int_{t-\frac{T}{2}}^{t+\frac{T}{2}} L^2(t)\,dt\right]^{1/2} \qquad (1)$$

where T is taken as a period of 1/2 second. This value was computed at successive overlapping 2/10-second intervals and each value is plotted in figure 3 at the time corresponding to the middle of the 1/2-second period. A 1/2-second period, involving the root mean square of 50 measured values, was selected after some trial as being long enough to give a sample of reasonable stability in a statistical sense, yet short enough to reflect changes in level associated with changes in flight condition.

Stall regime, run A.- For readier comparison of the buffet intensity with airplane operating condition in the stall, the data of figure 2(a) have been replotted in figures 3(a) and (b) as $\sigma(t)$ against both C_N and α. In these plots the square symbols are used to distinguish the data applicable to the stall recovery ($t > 5$ seconds in figure 2(a)). No particular trend of wing or tail buffet load with C_N is evident in figure 3, or of wing buffet load with α, but a possible correlation of tail buffet load with α is indicated. In an attempt to decide on an objective basis whether the scatter shown in figure 3 was larger than could reasonably be ascribed to chance, and thus might indicate the presence of some systematic factor in the data, a standard statistical test (Bartlett's, ref. 8) for homogeneity was applied to the values of $\sigma(t)$. For the wing loads (fig. 2(a)) this test suggests that the scatter shown is within the limits to be expected on the basis of chance, but the scatter for the tail loads is greater than would be expected on the basis of chance alone. This finding, together with the apparent correlation of tail load with angle of attack, tends to confirm the indications of reference 3 that "one or more additional parameters may exist which are important in determining tail loads but which are not disclosed by the present investigation."

Shock regime, run B.- In figure 2(b) the time histories of σ show marked similarities to the time history of C_N. These values of buffet intensity are compared directly with C_N in figure 4(a). Both wing and tail loads increase sharply with values of C_N above about 0.46. The

trend appears to be well represented by the least-squares straight lines shown which fit the wing and tail loads with standard errors of estimate of 36 and 18 pounds, respectively. In fitting these lines, the data represented by flagged symbols were omitted. These data apply to the rapid return to level flight ($t > 4$ seconds) in run B, where conditions were changing too rapidly to be represented adequately by 1/2-second averages.

Because of extraneous factors, the values of σ in figure 4(a) do not go to zero. For the wing data, the random errors associated with record reading, combined with strain-gage sensitivity (16,000 lb/in.), had a standard deviation of about 60 pounds. For the tail loads, reading accuracy was not a factor, but a periodic component is always present in the tail-load record at the propeller blade passage frequency, 86 cps. This component of the tail load in level flight in run B has a root-mean-square value of about 25 pounds, and an examination of the original records shows that it increases somewhat with lift. These effects tend to obscure the detail in resolving low levels of buffeting, but they are judged not to affect appreciably the larger values of $\sigma(t)$.

Although it appears that a plot of the variation of buffet intensity with C_N at a given Mach number could be used to determine the value of C_N at which buffeting starts, and thus to find a point on the buffet boundary, application of this concept is complicated in the present instance by both the decrease in Mach number during the run and by the extraneous effects mentioned previously which have obscured the buffet loads of low magnitude. It does appear, however, that buffeting is present at values of C_N greater than 0.46, a value which compares favorably with the condition for onset of buffeting indicated in figure 1.

In order to correlate the variations of buffet load with both C_N and Mach number in the shock regime, a penetration parameter P was defined in reference 3. A given value of C_N at a given Mach number, which penetrated the buffet region by an increment $C_N - C_{N_{BB}}$, was expressed as a ratio in terms of the maximum possible penetration $C_{N_{max}} - C_{N_{BB}}$:

$$P = \frac{C_N - C_{N_{BB}}}{C_{N_{max}} - C_{N_{BB}}} \tag{2}$$

This formula takes care of variations of both C_N and Mach number. The buffet loads of run B are plotted against P in figure 4(b). The variation with P appears to be linear. Least-squares straight lines through

the origin fit the wing and tail load data with standard errors of estimate of 32 pounds and 14 pounds, respectively. As before, data represented by the flagged symbols were omitted in fitting the least-squares straight lines.

ANALYSIS AND DISCUSSION

Method of Analysis

As discussed in appendix A, assessment of the Gaussian or non-Gaussian character of the measured flight buffet loads in terms of the usual formal definition of Gaussian random processes would involve a set of related probability distributions, most of which would be difficult to determine or to visualize. In the present paper, only the simplest of these distributions is used directly for comparison with the measured loads. The other properties to be examined follow from the nature of these probability distributions, but are determined from the power spectrum of the loads. The power spectrum $\Phi(f)$ may be regarded as a frequency analysis of the mean-square value of the load fluctuations. The equations for the properties used specifically in the present study follow.

The standard deviation σ or root-mean-square value is determined by the area under the power spectrum as

$$\sigma^2 = \int_0^\infty \Phi(f)\, df \tag{3}$$

The number of crossings per second of the zero axis with positive (or negative) slope is an average frequency f_0 where

$$f_0^2 = \frac{\int_0^\infty f^2 \Phi(f)\, df}{\int_0^\infty \Phi(f)\, df} \tag{4}$$

The total number of positive (or negative) peaks per second is f_p, where

$$f_p^2 = \frac{\int_0^\infty f^4 \Phi(f)\, df}{\int_0^\infty f^2 \Phi(f)\, df} \tag{5}$$

The probability distributions of the loads and of the load peaks are most conveniently expressed in terms of the so-called standard variable $z = \frac{L}{\sigma}$ which expresses the size of a given value of load L in relation to the standard deviation σ. The probability that L lies between L and $L + dL$ is $\frac{W_1(z)\,dL}{\sigma}$, where

$$W_1(z) = \frac{1}{\sqrt{2\pi}} e^{-z^2/2} \tag{6}$$

is the normal frequency distribution of statistics or the "normal curve of error." The probability of exceeding, that is, $P_N(L)$, is expressed by an integral of equation (6) as the normal probability distribution function

$$P_N(z) = \int_{z=L/\sigma}^{\infty} W_1(z)\,dz \tag{7}$$

a relation which may be evaluated by use of standard statistical tables.

The probability that a peak load will exceed a given value L, that is, $P_P(L)$, is expressed by a peak probability distribution function $P_P(z)$ where

$$P_P(z) = P_N\left(\frac{z}{k_1}\right) + \frac{f_0}{f_p} e^{-z^2/2}\left[1 - P_N\left(\frac{z}{k_2}\right)\right] \tag{8}$$

and the constants k_1 and k_2 are functions of the ratio f_0/f_p,

$$k_1 = \sqrt{1 - \left(f_0/f_p\right)^2} \tag{9}$$

$$k_2 = \frac{k_1}{f_0/f_p} \tag{10}$$

Equation (8) is illustrated in figure 5(a) for various values of the frequency ratio f_0/f_p. For the limiting case $f_0/f_p = 0$, the peak probability distribution $P_P(z)$ reduces to the normal distribution (eq. (7)). This figure has been prepared on normal-probability paper - paper on which the scales are so adjusted that the normal probability distribution gives a straight-line plot and which thus serves to illustrate the relationship between the normal and peak probability distributions.

In a Gaussian random process, the first member of the aforementioned set of related probability distributions can be represented by the normal probability distribution, equation (7). The Gaussian character of the buffet loads in the present paper is, therefore, first assessed by comparing equation (7) with the probability distribution of the measured load time histories taken from the flight records. In addition, the distribution of the peaks is compared with equation (8), and the values of f_0 and f_p determined by counting are compared with the values obtained from the power spectrum by using equations (4) and (5). Inasmuch as the power spectrum is so closely involved in these comparisons, the frequency characteristics of the loads measured in the present study are discussed prior to the probability characteristics.

Power Spectrum of Buffet Loads

The frequency content of the wing and tail loads measured in runs A and B is shown in figure 6. These power spectra were computed from the load time histories by use of the numerical techniques devised by Tukey, as outlined in reference 7. Since the spectra are based on sample time histories of finite length read at discrete time intervals ($\Delta t = 0.01$ second), they represent certain necessary compromises with regard to frequency range, resolution, and precision. These compromises are discussed in detail in reference 7. The spectra, therefore, should be considered as estimates of the power spectral density functions of the buffet loads rather than true power spectral densities.

The power spectra of figure 6 are essentially characteristic of the random response of a lightly damped single-degree-of-freedom system. The location of the large peak at low frequencies in the wing-load spectra correlates well with the frequency of first symmetric bending, 9.3 cps (table I) for the modified airplane (fig. 6(a)) and 11.7 cps for the basic airplane (fig. 6(c)), and thus reflects the change in frequency characteristics associated with the added wing-tip weights. The first assymmetric bending mode and first torsion mode also appear in the wing spectra but these contributions are small. The larger low-frequency peak in the tail spectra appears to reflect the fuselage in a torsion, or "tail rocking," mode at 9.8 cps; identification of the other low peaks in terms of known structural modes is less certain.

Probability Distribution of Buffet Loads

As a first step in assessing the Gaussian character of the random loads represented by the power spectra of figure 6, the number of values from the load time history that fall in various class intervals are given in table II. Similar frequency-distribution data are given in table III for the load ratio L/P, a simple transformation of the buffet

load suggested by the strong linear dependence of load on penetration beyond the buffet boundary shown in figure 4(b). The "Loads" columns of tables II and III were obtained by sorting into the appropriate classes the punched cards containing the time histories of load or of transformed load. Also given in the tables is the mean value of each frequency distribution and the standard deviation σ.

The probability of exceeding a given value of L or of L/P, based on the load frequency data of tables II and III, is shown in figures 7 and 8. These figures have been prepared on normal-probability paper. Since the normal probability distribution $P_N(L)$ (eq. (7)) gives a straight-line plot, use of probability plotting paper constitutes one of the simplest qualitative tests for a normal distribution. For the shock regime, run B, the distributions of both L_w and L_t (fig. 7) have excessive occurrences of very large and very small values as compared with a normal distribution. For the stall regime, run A, the normal distribution is a representation of the data which would be adequate for most engineering purposes, although it is somewhat better for the wing loads than for the tail loads. The transformed loads for wing and tail L/P (fig. 8) correspond even more closely to the normal distribution than do the stall loads of run A.

A standard statistical test of the significance of such differences between an observed distribution and an assumed distribution as are evident in figures 7 and 8 is provided by the χ^2 (chi-square) test. (See, for example, ref. 8.) The numerical quantities required for the use of this test are given at the bottom of tables II and III. Included are the value of χ^2 and for comparison the value $\chi^2_{.05}$, which is the value of χ^2 at the 5-percent level of significance. In accordance with usual practice, a calculated value of χ^2 less than that for the 5-percent level of significance may be regarded as indicating that the differences between the observed distribution and the normal distribution are not significant. On the basis of the qualitative comparison of figures 7 and 8 and on the more objective basis of the chi-square test, it is concluded that the buffet loads in the stall regime and the transformed loads in the shock regime display one important characteristic of a Gaussian random process, normality of the first probability distribution.

Probability Distribution of Peak Buffet Loads

For comparison with the peaks of a Gaussian random process, the frequency distributions of the buffet-load peaks of runs A and B are given in table II and the peaks of the transformed loads are given in table III. The frequencies of both positive and negative peaks are tabulated. The distinction between positive and negative peaks is based

not on the relative position of the zero axis, but on the usual definitions of the maximums and minimums of a continuous function. Thus a peak occurs when the first derivative of a function is zero; it is a positive peak when the second derivative is negative (positive curvature) and it is a negative peak when the second derivative is positive.

The peak probability distributions corresponding to the peak data of tables II and III are plotted in figure 9. The abscissa in this figure is the standard variable z, equal to L/σ, or, in the case of the transformed load, $\frac{L/P}{\sigma}$. The probability $P_p(z)$ is the probability that a peak will exceed a given value of z. For the purposes of figure 9, the negative peak distributions of each load were inverted about the zero axis and combined with the corresponding positive peak distributions to give an average or effective peak distribution. This procedure was adopted to simplify the presentation and to increase the size of the comparatively small samples, since there appeared to be no special differences between the positive and negative distributions.

For comparison of an observed peak distribution with the peak distribution of a Gaussian random process, a value of the ratio f_0/f_p is required for use in equation (8). The lines plotted in figure 9 represent the peak probability distribution function $P_p(z)$ (eq. (8)) for two estimates of the ratio f_0/f_p. The solid lines are for the values obtained by counting zero crossings and peaks in the time history; the dashed lines represent values obtained from the respective power spectra of the load by use of equations (4) and (5). The numerical values involved are summarized in table IV. The spectrum values of f_0/f_p average 0.12 smaller than the corresponding time-history values but the effect of this difference on the shape of the peak distribution is small, especially at the level of the larger, more infrequent peaks. For the loads which had a Gaussian first probability distribution (run A and the transformed loads of run B) the observed peak probability distributions appear to be in good agreement with the theoretical distribution. For run B, which had loads that were not normally distributed, the peak distribution appears to reflect the excess of very large and very small values. The qualitative results of this comparison are confirmed by the chi-square test, for which the pertinent numerical data are given at the bottom of the peak frequency columns of tables II and III. The values of χ^2 shown for the peak loads of run A and the transformed peak loads of run B are not significant at the 5-percent level. These distributions are, therefore, judged to display another characteristic of a Gaussian random process; that is, the probability that a peak will exceed a given value is given by the peak probability distribution for a Gaussian process. The test was not applied to the peak loads of run B in table II in view of the nonstationary character of the loads prior to transformation and the large departures of the peak distributions shown in figure 9.

In table IV the values of f_0 and of f_p obtained by use of equations (4) and (5) from the power-spectrum estimates of runs A and B are compared with the values actually observed. The spectrum value of the zero-crossing frequency exceeded the observed time-history value by 1.8 to -0.6 cps. The estimates of peak frequency f_p from the power spectra exceeded the time-history values by amounts ranging from 5.3 to 8.6 cps, or as much as 33 percent. Values of f_0 are thus obtained from the spectrum more accurately than are the values of f_p. For the purpose of load prediction, the frequency of the larger loads is primarily determined by the value of f_0, and the agreement between the values of f_0 shown in table IV is considered satisfactory. The fact that the spectrum values of f_p are consistently larger than the observed values may perhaps indicate some non-Gaussian character of the buffet process which is appearing in the second derivative. On the other hand, inaccuracies in the power estimates at the higher frequencies which do not greatly affect the precision of the value of σ can be magnified by differentiation (eq. (A24)) and can thus affect the accuracy with which the spectrum of the second derivative can be obtained by this method. Although the apparent deviation from the Gaussian distribution which is evident in the second derivative is of considerable theoretical interest and appears to warrant further investigation, for most practical purposes buffeting can be treated as a Gaussian random process.

Application of Present Results to Buffet Research

Two results of the present study are of special interest in connection with the investigation of buffeting. These results have to do with the Gaussian character of the loads and with the simplicity of the power spectral densities of the loads.

The Gaussian character of the loads is significant in view of the wealth of statistical information available about Gaussian distributions as outlined in the section entitled "Method of Analysis" and in appendix A. As applied to buffeting, such statistical properties as the percentage of time a given load is exceeded, the number of cycles, and the magnitude of peaks are perhaps of most interest since they have immediate application in connection with estimation of limit loads and fatigue effects.

The power spectral densities of the loads measured in the present study may be considered as the resultant of a random fluctuating input acting on an elastic system. As outlined in references 2 and 3, the characteristics of output, input, and system may be expressed in terms of three related frequency functions as

$$\Phi_o(f) = A^2(f)\Phi_i(f)$$

where

$\Phi_i(f)$ frequency content of input force

$\Phi_o(f)$ frequency content of the output or response (structural load, displacement, velocity, acceleration, etc.)

$A^2(f)$ square of the admittance of the system to a sinusoidal force

Buffeting is thus expressed in terms of three pertinent quantities, each of which may be investigated independently. Since an airplane, vibrationwise, is a very complex system, the admittance could conceivably be a complex expression involving many degrees of freedom. It is in this connection that the simple power spectra shown in figure 6 are significant. Each spectrum reflects predominantly the response of a single degree of freedom - in the case of the wing, the first symmetric bending mode. As illustrated in references 2 and 3, restriction to a single degree of freedom can lead to some simple analytical results. In the case of the present unswept wing, it appears that such a restriction, as exemplified in appendix B of reference 3, should permit the determination of first-order effects at least. In view of the bending-torsion coupling which is characteristic of swept wings, the admittance of swept wings is possibly more complex than that of unswept wings, and a study of the power spectral densities of other plan forms would be of interest.

Correlation With Previous Results

Inasmuch as the present study stems from the study of peak buffet loads reported in reference 3, and was undertaken partly to investigate some of the assumptions made in that analysis, a comparison of some of the present results with those of reference 3 is indicated. In the analysis of the peak wing buffet loads reported in reference 3, use was made of an asymptotic expression for the peak probability distribution of a Gaussian process, obtained in reference 4 (eq. 3.6-11) and given in appendix A of the present paper as equation (A35). This expression, for the number of positive (or negative) peaks per second N_L which exceed a value of L, is

$$N_L \approx f_0 e^{-L^2/2\sigma^2} \tag{11}$$

Equation (11) applies almost exactly to peaks larger than 1 standard deviation. Alternatively, the peak value ΔL, which will occur only once in a period T, is obtained by solution for ΔL of the equation

$$f_0 T = e^{\Delta L^2/2\sigma^2} \tag{12}$$

As an estimate of f_0, the value used in reference 3 was the frequency of first symmetrical wing bending, the dominant mode in wing buffeting. This frequency was 11.7 cps for run B. The probability distribution of the peak wing loads of run B, expressed as L/P, is plotted in figure 10, in comparison with the asymptotic expression for these loads. The lines represent three different values of f_0. The line marked 11.7 cps corresponds to the assumptions of reference 3, 14.8 is the value of f_0 counted (table IV), and 16.4 cps is the spectrum value (eq. (4)). Each of the lines is a fair representation of the data. The differences between them would be of little practical significance in such fields as fatigue, where differences of 2 to 1 in such quantities as fatigue life are to be expected.

For the random response of a linear single-degree-of-freedom oscillator subject to a Gaussian random input with a white spectrum, the zero crossing frequency f_0 is equal to the undamped natural frequency. The difference between 9.3 cps for run A, 11.7 cps for run B, and the values of f_0 given in table IV may be considered as the effects of the presence of other structural modes in the buffet loads (fig. 6) and of departures of the color of the unknown buffet input spectrum from white; nonetheless, it appears from figure 10 that a single-degree-of-freedom approximation would account at least for first-order effects.

In the present paper, use of the root-mean-square buffet loads over short intervals, as in figures 2, 3, and 4, has resulted in efficient use of flight-test results. In the analysis of reference 3, only one datum point was obtained for each run, since the measure of buffet load was ΔL, one-half of the largest peak-to-peak fluctuation measured in the run. The statistical nature of the relationship between the standard deviation or root mean square and the peak values makes possible a comparison of the results obtained with the two measures. In reference 3 the analysis of the wing loads in 26 runs led to the relation

$$\Delta L_W = (153.5 \pm 6.4)P\sqrt{q} \tag{13}$$

The slope of the least-squares line through the wing data of figure 4(b) is 672 ± 25 pounds per unit change in penetration which, taken with a value for q of 292 pounds per square foot, leads to

$$\sigma_W = 39P\sqrt{q} \tag{14}$$

The 26 maneuvers analyzed in reference 3 averaged 4.6 seconds in duration. If f_0 is taken as 14.8 cps (table IV), equation (12) indicates that on the average not more than one peak in 4.6 seconds would exceed the standard deviation by a factor of 2.92, or

$$\Delta L_W \approx 2.92\sigma_W$$
$$\approx 114P\sqrt{q} \qquad (15)$$

The results for run B are therefore within about 30 percent of the results obtained for the 26 runs of reference 3. The agreement would have been closer had the values of P used for the correlation of reference 3 been the largest penetration rather than the sometimes smaller actual value at the time the peak load was obtained, but the results from the two different measures of buffet intensity can be considered in good agreement. Whereas the standard deviation makes more efficient use of the data and utilizes a measure of greater stability, more computational effort is required to obtain it than the simpler peak-to-peak values. However, either technique could be used, the standard deviation being the preferred measure when flight-test time must be conserved.

CONCLUDING REMARKS

Some statistical properties of the buffet loads measured on the wing and tail of a fighter airplane have been analyzed in an attempt to determine whether buffeting can be considered a Gaussian random process.

For a representative stall maneuver it appears that the wing buffeting is essentially a Gaussian random process. The loads are normally distributed, and the probability that a load peak will exceed a given level is in agreement with the theoretical results obtained by Rice in "Mathematical Analysis of Random Noise." There is evidence that the tail buffet loads are not so normally distributed as the wing loads, and there is also some evidence of correlation between angle of attack and tail buffet intensity.

For a representative pull-up into buffeting in the shock regime, the buffet intensity appears to vary linearly with penetration beyond the buffet boundary. The loads under maneuvering conditions are therefore not stationary and are thus non-Gaussian, but by means of a simple linear transformation the buffet loads in maneuvering flight can be treated as a Gaussian process.

The power spectrum of the wing root shear indicates that buffet shear loads are primarily associated with response in the first symmetrical bending mode. Although other structural modes are present, their contribution is small, and the spectrum is essentially characteristic of the response of a lightly damped single-degree-of-freedom system to a random disturbance. The power spectrum of the tail root shear indicates that the tail loads are primarily associated with the fuselage in a torsion, or "tail-rocking," mode.

In studies of the relationship between buffeting intensity and airplane operating conditions, numerical filtering techniques have been found effective for separating the buffet loads from the low-frequency load components associated with the maneuvering of the airplane. A useful measure of buffet intensity was the root-mean-square buffet shear averaged over a 1/2-second interval. This measure was found to be sufficiently stable statistically, yet did not encompass so long an interval that the effects of changes in flight condition were obscured.

Langley Aeronautical Laboratory,
National Advisory Committee for Aeronautics,
Langley Field, Va., May 10, 1956.

APPENDIX A

SOME CHARACTERISTICS OF A GAUSSIAN RANDOM PROCESS

The nature of some of the concepts available for the description of random processes and the simplifications which result when the process is Gaussian are discussed in this appendix. Emphasis is given to some of the practical applications of items which are developed in more detail in references 4, 5, 6, and 7. The discussion is restricted to what is termed a "stationary" random process. For random time series such as are dealt with in the present paper, the restriction to stationary means that while the quantity of interest (for example, load) varies with time, the value of any statistical measure of the quantity (for example, its mean square) does not depend upon the time for which the measure is determined. Thus time does not enter directly, but is used only as a means of specifying the duration of a time interval.

Probability Distributions

A stationary random function of time $y(t)$ may be characterized by a series of related probability functions W_1, W_2, . . . W_n where

$W_1(y)\,dy$ is the probability of finding y between y and $y + dy$;

$W_2(y_1,y_2,\tau)\,dy_1\,dy_2$ is the joint probability of finding a pair of values of y in the ranges y_1 to $y_1 + dy_1$ and y_2 to $y_2 + dy_2$, which are a time interval τ apart from each other;

$W_3(y_1, y_2, y_3,\tau_1,\tau_2)\,dy_1\,dy_2\,dy_3$ is the joint probability of finding a triple of values of y in the ranges y_1 to $y_1 + dy_1$, y_2 to $y_2 + dy_2$, and y_3 to $y_3 + dy_3$, where dy_1 and dy_2 are the time interval τ_1 apart and dy_2 and dy_3 are the time interval τ_2 apart.

The W_n probability distributions represent a complete statistical description of the process, each distribution of higher order describing it in greater detail. The function $W_1(y)$ is termed the first probability density; it fulfills the requirements that a probability function is never negative, and that

$$\int_{-\infty}^{\infty} W_1(y)\,dy = 1 \qquad \text{(A1)}$$

It also serves to define the probability function $P(y)$, which is the probability that a given value of y will be exceeded; that is

$$P(y) = \int_{y}^{\infty} W_1(y)\, dy \tag{A2}$$

From $W_1(y)$ the average value of y can also be found:

$$\bar{y} = \int_{-\infty}^{\infty} y\, W_1(y)\, dy \tag{A3}$$

which (for a stationary random process) is the same as the time average $\bar{y} \equiv \lim_{T \to \infty} \frac{1}{2T} \int_{-T}^{T} y(t)\, dt$.

A measure of the spread of the values of $y(t)$ around the average value $\bar{y}$ is the standard deviation σ, which is defined as the square root of the average value of $(y - \bar{y})^2$:

$$\sigma = \left[\overline{(y - \bar{y})^2}\right]^{1/2} \tag{A4}$$

The value of σ may also be obtained from $W_1(y)$ as

$$\sigma^2 = \int_{-\infty}^{\infty} (y - \bar{y})^2\, W_1(y)\, dy \tag{A5}$$

For many purposes it is convenient to express y in terms of its fluctuations about the average value, normalized by the standard deviation. Such a dimensionless expression is denoted by the standard variable z, where

$$z = \frac{y - \bar{y}}{\sigma} \tag{A6}$$

When changing variables from y to z, a dual change of scale is involved with probability densities, since the fundamental requirement of a probability distribution must be observed; that is,

$$\int_{-\infty}^{\infty} W_1(y)\, dy = \int_{-\infty}^{\infty} W_1(z)\, dz = 1 \tag{A7}$$

and hence

$$W_1(z) = W_1(y) \frac{dy}{dz} = \sigma W_1(y) \tag{A8}$$

From the second probability distribution, W_2, is obtained the mean value of the product $y(t)\, y(t+\tau)$ where τ is the difference in time between the values of y. This mean value

$$\overline{y_1 y_2} = \iint y_1 y_2 W_2(y_1, y_2, \tau)\, dy_1\, dy_2 \tag{A9}$$

which is a function of τ, is the same (for a stationary process) as the time average

$$\overline{y(t)\, y(t+\tau)} = \lim_{T \to \infty} \frac{1}{2T} \int_{-T}^{T} y(t)\, y(t+\tau)\, dt \tag{A10}$$

It gives a measure of the correlation between values of y separated by a time interval τ and is termed the correlation function $R(\tau)$ of the random process. From equation (A10) when $\tau = 0$ it is evident that

$$R(0) = \overline{y^2} \tag{A11}$$

For conformity with standard statistical practice where perfect correlation is denoted by a value of 1, the correlation function may be normalized and expressed as

$$\rho(\tau) = \frac{\overline{\left[y(t) - \bar{y}\right]\left[y(t+\tau) - \bar{y}\right]}}{\overline{\left[y(t) - \bar{y}\right]^2}} \tag{A12}$$

Power Spectrum

The information contained in the W_n probability distribution functions is also contained in a set of distribution functions which describe the frequency content of the time variations of the random function $y(t)$. The simplest of these frequency distribution functions is generally called the power spectrum or power spectral density and in this paper is denoted by the symbol $\Phi(f)$. Under suitable limitations (see, for example, ref. 6, sec. 6.7), $\Phi(f)$ can be defined in terms of a Fourier transform of the random time function $y(t)$, but frequently of more practical interest is the relationship with the correlation function $R(\tau)$ expressed in the Fourier cosine transform pair

$$\Phi(f) = 4\int_0^\infty R(\tau) \cos 2\pi f\tau \, d\tau \tag{A13}$$

$$R(\tau) = \int_0^\infty \Phi(f) \cos 2\pi f\tau \, df \tag{A14}$$

Equation (A13) is the basis for most numerical methods of obtaining $\Phi(f)$. From equation (A14) when $\tau = 0$ a relation follows between power spectral density and the mean square:

$$\int_0^\infty \Phi(f) \, df = R(0) = \overline{y^2} \tag{A15}$$

Thus the power spectrum may be regarded as a frequency analysis of the mean square value of the random time function. The function $\Phi(f)$ when applied to a random process is regarded as a continuous function, in distinction to, say, Fourier coefficients which convey similar information about the amplitudes of harmonic functions. In the event that a time function contains nonrandom elements such as a mean level (in electrical terms, a direct-current component) or periodic components such as $A_k \sin\left(2\pi f_k t - \alpha_k\right)$, the spectrum will contain discontinuous peaks. This information can, however, be expressed in continuous form through the convention of the Dirac delta function $\delta(f-f_k)$, defined as

$$\left.\begin{aligned} &\delta(f-f_k) = 0 \qquad (f \neq f_k) \\ &\int_{-\infty}^{\infty} \delta(f-f_k) \, df = 1 \end{aligned}\right\} \tag{A16}$$

Also, $\delta(f) = \delta(-f)$ and hence

$$\int_0^\infty \delta(f) \, df = \frac{1}{2} \tag{A17}$$

With this convention, for a time function

$$y(t) = \overline{y} + A_k \sin\left(2\pi f_k t - \alpha_k\right) \tag{A18}$$

the correlation function is

$$R(\tau) = \overline{y}^2 + \frac{A_k^2}{2} \cos 2\pi f_k \tau \tag{A19}$$

and the power spectrum is

$$\Phi(f) = 2\overline{y}^2\delta(f) + \frac{A_k^2}{2}\delta(f-f_k) \tag{A20}$$

These relationships are frequently of use in analyzing the characteristics of experimentally derived spectra.

The Gaussian Random Process

A stationary random process is termed Gaussian provided all members of the set of multidimensional probability distributions W_n are Gaussian This requirement means that the first probability distribution $W_1(y)$ may be expressed functionally as

$$W_1(y) = \frac{1}{\sigma\sqrt{2\pi}} e^{-(y-\overline{y})^2/2\sigma^2} \tag{A21}$$

This equation represents a one-dimensional Gaussian distribution, the so-called normal distribution of statistics. The second probability distribution $W_2(y_1,y_2,\tau)$ is a two-dimensional Gaussian distribution which involves the normalized correlation function $\rho(\tau)$:

$$W_2(y_1,y_2,\tau) = \frac{1}{2\pi\sigma^2\sqrt{1-\rho^2}} e^{-\frac{y_1^2+y_2^2-2\rho y_1 y_2}{2\sigma^2(1-\rho^2)}} \tag{A22}$$

and in general the W_n probability distribution is an n-dimensional Gaussian distribution.

The definition of a Gaussian random process in terms of such a set of n-dimensional Gaussian distributions, although complete, is hardly a definition of practical utility. Its importance stems from the fact that for the Gaussian random process all of the distributions W_n will depend only on σ^2 and $\rho(\tau)$, two quantities which in turn are derived from the power spectrum, as in equations (A13) and (A15). Therefore, the spectral density $\Phi(f)$ may, with equation (A21), be regarded as a basic description of a Gaussian random process. Other characteristics of a Gaussian

process follow from the relationship between the power spectrum and the W_n Gaussian probability distributions. Of considerable practical interest in this connection are the relationships between the power spectrum, the derivatives of $y(t)$, the frequency of zero crossings, and the frequency of occurrence of peaks in the time history.

Derivatives of a Gaussian random process.- A consequence of the Gaussian character of a random time function $y(t)$ is the relationships between the derivatives of $y(t)$ and the power spectral density $\Phi(f)$:

$$\overline{\dot{y}(t)^2} = \int_0^\infty (2\pi f)^2 \Phi(f)\, df = \sigma_{\dot{y}}^2 \tag{A23}$$

and

$$\overline{\ddot{y}(t)^2} = \int_0^\infty (2\pi f)^4 \Phi(f)\, df = \sigma_{\ddot{y}}^2 \tag{A24}$$

It can also be shown that the correlation between $y(t)$ and its derivatives is

$$\left.\begin{aligned} \overline{y(t)\dot{y}(t)} = 0 = \overline{\dot{y}(t)\ddot{y}(t)} \\ \text{and} \\ \overline{y(t)\ddot{y}(t)} = -\overline{\dot{y}(t)^2} \end{aligned}\right\} \tag{A25}$$

For some analytic frequency functions $\Phi(f)$ which are satisfactory representations of certain physical processes over the frequency range of usual interest, equations such as (A23) or (A24) would have no meaning, since the integrals would not converge. However, it appears that for physical systems parasitic effects will always be present at sufficiently high frequencies, and $\Phi(f)$ will always approach zero rapidly enough so that the integrals will converge.

Peak values of a Gaussian process.- In part III of reference 4 a number of results are obtained on the distribution of the zeros, of the maximums or peaks, and of the envelope of a Gaussian time function. The relations for the number of zeros and for the number and probability distribution of the peaks are of special interest, because they are easily determined from a time-history record and from the power spectrum and because they are quantities which enter directly into the study of fatigue. The number of times per second that the zero axis is crossed with positive (or negative) slope is, on the average,

$$f_0 = \frac{1}{2\pi} \frac{\sigma_{\dot{y}}}{\sigma_y} \tag{A26}$$

and the total number of positive (or negative) peaks is

$$f_p = \frac{1}{2\pi} \frac{\sigma_{\dot{y}}}{\sigma_{\dot{y}}} \tag{A27}$$

Equations (A26) and (A27), together with equations (A15), (A23), and (A24), lead to equations (4) and (5) of the present study. The ratio f_0/f_p is the negative of the coefficient of correlation between y and $\ddot{y}$. The probability $W_p(y)\,dy$ that a positive peak will fall between y and $y + dy$ is given by a peak probability density function which, in terms of the standard variable z, is

$$W_p(z) = \frac{k_1}{\sqrt{2\pi}} e^{-z^2/2k_1^2} + \frac{f_0}{f_p} z e^{-z^2/2} \left(1 - P_N \frac{z}{k_2}\right) \tag{A28}$$

where

$$k_1 = \sqrt{1 - \left(\frac{f_0}{f_p}\right)^2} \tag{A29}$$

$$k_2 = \frac{k_1}{f_0/f_p} \tag{A30}$$

and $P_N\left(\frac{z}{k_2}\right)$ is the normal probability that a value z/k_2 will be exceeded; that is,

$$P_N\left(\frac{z}{k_2}\right) = \frac{1}{\sqrt{2\pi}} \int_{y/k_2\sigma}^{\infty} e^{-z^2/2}\,dz \tag{A31}$$

Equation (A28) is essentially equation (3.6-5) of reference 4 expressed in the notation of the present paper. The frequency ratio f_0/f_p is the parameter which determines the shape of $W_p(z)$; equation (A28) is plotted in figure 5(b) for several values of the ratio f_0/f_p. For the limit of $f_0/f_p = 0$, the distribution reduces to the normal distribution; for the upper limit of $f_0/f_p = 1$, the distribution reduces to the Rayleigh distribution.

Equation (A28) has been integrated to obtain the probability $P_P(y)$ that, of all the positive (or negative) peaks of a Gaussian random process, a peak chosen at random will exceed a given value of $y = z\sigma$. The resulting expression

$$P_P(y) = \int_{y/\sigma}^{\infty} W_P(z)\, dz$$

$$= P_N\left(\frac{z}{k_1}\right) + \frac{f_0}{f_p} e^{-z^2/2}\left[1 - P_N\left(\frac{z}{k_2}\right)\right] \tag{A32}$$

is plotted in figure 5(a); it is a function of normal probability distributions and the ratio f_0/f_p.

The actual number of positive peaks per second which would exceed a given value of $y = z\sigma$ is, on the average, N_z, where

$$N_z = f_p\, P_P(z) \tag{A33}$$

As pointed out in reference 4, an asymptotic expression for the peak probability density, equation (A28), is

$$W_P(z) \approx f_0 z e^{-z^2/2} \tag{A34}$$

an expression which is quite accurate for $z > 1$ or $y > \sigma$. The corresponding expression for the number of positive peaks per second which exceed a given value of z is, from equations (A32) and (A33),

$$N_z \approx f_0 e^{-z^2/2} \tag{A35}$$

This is a convenient expression which plots as a straight line on semilogarithmic paper when z^2 is used as the abscissa.

APPENDIX B

NUMERICAL FILTERING

The load time histories recorded in the present investigation can be considered to be composed of a maneuver component and a buffet component. The frequency content of the maneuver was concentrated in the vicinity of the frequency of the short-period pitching motion (about 1 cps) while the principal components of the buffeting were of the order of 10 to 12 cps. For separation of the buffet component, some method of discrimination between components above and below about 3 to 4 cps was desired. Estimation of the maneuver component by means of a manually faired mean line and measurement of the buffet component relative to this line was tedious and uncertain. Estimation of the maneuver component by calculation of the running mean proved to be a simple numerical procedure, but use of the running mean is equivalent to use of a low-pass numerical filter with a long tail and systematic phase shifts which were undesirable. A special high-pass numerical filter was therefore devised which is suitable for use with punched-card equipment, has no phase shifts, and has a sharply defined cutoff in the desired frequency range. The filter was, in effect, based on the properties of a particular class of low-pass, high-pass, and band-pass numerical filters. Since the approach used can be extended to the development of other filters with a wide range of characteristics, and since it differs in some respects from the method used in reference 9, it is described in some detail.

Frequency Characteristics of Numerical Data

For application of numerical procedures, a continuous function of time $y(t)$ is ordinarily reduced to discrete time-history form y_i by sampling at the uniform time interval Δt. This new function y_i is thus defined at the particular values of

$$t = i\,\Delta t \qquad (i = 0, 1, 2, \ldots) \qquad \text{(B1)}$$

but is undefined at intermediate values. There is no loss of information in this reduction if $y(t)$ contains no components with frequencies greater than a frequency f_F, termed the Nyquist frequency or folding frequency, where

$$f_F = \frac{1}{2\,\Delta t} \qquad \text{(B2)}$$

The folding frequency has the property that in any frequency representation of $y(t)$, determined from the values of y_i, components of

frequency f, $(2f_F \pm f)$, $(4f_F \pm f)$, and so forth, cannot be distinguished. Thus components of such frequencies greater than f_F appear in the frequency representation at the frequency f in the range $0 \leqq f \leqq f_F$, and the whole range of frequencies in $y(t)$ has been folded into the range 0 to f_F. This folding property follows from the relations

$$\sin 2\pi(2f_F \pm f)t = \sin(2\pi i \pm 2\pi ft) = \pm \sin 2\pi ft$$

$$(i = 0, 1, 2, \ldots)$$

Binomial-Coefficient Filters

The binomial coefficients $\binom{n}{k}$ as displayed in the array

n \ k	0	1	2	3	4	5	6	7	8	...	n - 1	n
1	1	1										
2	1	2	1									
3	1	3	3	1								
4	1	4	6	4	1							
5	1	5	10	10	5	1						
6	1	6	15	20	15	6	1					
7	1	7	21	35	35	21	7	1				
8	1	8	28	56	70	56	28	8	1			
.	.	.	.	.	.	.	.	.	.			
n	1	n	... $\frac{n(n-1)(n-2)\ldots(n-k+1)}{k(k-1)(k-2)\ldots(3)(2)(1)}$							...	n	1

and their sums 2^n form the basis for a number of integrating and smoothing formulas. The smoothing action on numerical data is akin to the action of filters on electrical signals, as may be seen, for example, by considering the action of the formula based on $\binom{2}{k}$:

$$\bar{y}(t) = \frac{1}{2^2}\left[y(t-\Delta t) + 2y(t) + y(t+\Delta t)\right] \tag{B3}$$

when $y(t)$ is a sine wave of frequency f, that is

$$y(t) = \sin 2\pi ft$$

or, if $t = i\,\Delta t$,

$$y_i = \sin \frac{\pi f i}{f_F}$$

Application of the relation $\sin(a \pm b) = \sin a \cos b \pm \cos a \sin b$ to equation (B3) gives

$$\bar{y}(t) = \frac{1 + \cos(2\pi f\,\Delta t)}{2} \sin 2\pi ft$$

or

$$\bar{y}_i = \frac{1 + \cos \frac{\pi f}{f_F}}{2} y_i = \left(\cos^2 \frac{\pi}{2} \frac{f}{f_F}\right) y_i$$

Thus $\bar{y}(t)$ (or $\bar{y}_i$) is a sinusoid of the same frequency as $y(t)$ (or y_i) but the amplitude has been modified by the term $\cos^2 \frac{\pi}{2} \frac{f}{f_F}$, which thus represents the filter factor of the $\left(\frac{2}{k}\right)$ binomial-coefficient filter.

For data-processing purposes, the operation represented by equation (B3) is more conveniently expressed in matrix form as

$$\bar{y}_i = \frac{1}{4}\begin{bmatrix} 1 & 2 & 1 \end{bmatrix} \begin{Bmatrix} y_{i-1} \\ y_i \\ y_{i+1} \end{Bmatrix}$$

or, in general, for the nth-order binomial coefficients,

$$\bar{y}_i = \frac{1}{2^n}\left[\binom{n}{k}\right] \left\{y_i\right\} \tag{B4}$$

and the filter factor of the associated filter is easily shown to be

$$Y_n(f) = \cos^n \frac{\pi}{2} \frac{f}{f_F} \tag{B5}$$

Application of a second-order filter to obtain $\bar{y}_i$, followed by a repetition of this action on $\bar{y}_i$ to give $\bar{\bar{y}}_i$, is equivalent to a single application of a fourth-order filter, as may be seen from the matrix representation of this double filtering process:

$$\bar{\bar{y}}_i = \frac{1}{2^2}\begin{bmatrix}1 & 2 & 1\end{bmatrix}\begin{Bmatrix}\bar{y}_{i-1}\\ \bar{y}_i\\ \bar{y}_{i+1}\end{Bmatrix}$$

$$= \frac{1}{2^4}\begin{bmatrix}1 & 2 & 1\end{bmatrix}\begin{bmatrix}1 & 2 & 1 & 0 & 0\\ 0 & 1 & 2 & 1 & 0\\ 0 & 0 & 1 & 2 & 1\end{bmatrix}\begin{Bmatrix}y_{i-2}\\ y_{i-1}\\ y_i\\ y_{i+1}\\ y_{i+2}\end{Bmatrix}$$

$$= \frac{1}{2^4}\begin{bmatrix}1 & 4 & 6 & 4 & 1\end{bmatrix}\begin{Bmatrix}y_i\end{Bmatrix}$$

Successive operations of this type are commutative, use of an nth-order filter followed by an mth-order filter being equivalent to use of an (n+m)-order filter, and the filter factors are also commutative; that is,

$$Y_{(n+m)}(f) = Y_{(m+n)}(f) = \left(\cos \frac{\pi}{2}\frac{f}{f_F}\right)^{n+m} \qquad (B6)$$

The binomial filters are all low-pass filters, the filter factor being unity at $f = 0$ and zero at the folding frequency. The filters determined by the coefficients of even order have the special properties that they are nonnegative and have no phase shifts; thus, the time relationships of components of different frequencies are preserved. The low-pass-filter characteristic $Y_n(f)$ is plotted in figure 11(a) for the range $0 \leq \frac{f}{f_F} \leq 1$ for several even values of n. The higher the order of the filter, the sharper the low-frequency cutoff. As measured by the usual criterion of band width at the half-power point, $Y(f) = 0.707$, the second-order and 28th-order filters would have band widths of $0.36f_F$ and $0.10f_F$, respectively.

Modified Binomial Filters

By a simple operation on the coefficients, each even-order binomial filter can be related to a high-pass filter which has a filter factor

of 0 at $f = 0$ and 1 at the folding frequency. The time history $\bar{z}_i$ computed with the high-pass numerical filter is related to the time history $\bar{y}_i$ by the relation

$$\bar{z}_i = y_i - \bar{y}_i \tag{B7}$$

that is, the double operation - application of a low-pass filter followed by substraction from the original time history - is equivalent to a single operation with the related high-pass filter.

Since, from equations (B4) and (B7),

$$\bar{z}_i = y_i - \frac{1}{2^n}\left[\binom{n}{k}\right]\begin{Bmatrix} y_{i-(n/2)} \\ \vdots \\ y_i \\ \vdots \\ y_{i+(n/2)} \end{Bmatrix}$$

the coefficients for finding $\bar{z}_i$ in one operation are contained in the relation

$$\bar{z}_i = \frac{1}{2^n}\left[-\binom{n}{0} \quad -\binom{n}{1} \quad \cdots \quad 2^n - \binom{n}{n/2} \quad \cdots \quad -\binom{n}{n-1} \quad -\binom{n}{n}\right]\begin{Bmatrix} y_{i-(n/2)} \\ \vdots \\ y_i \\ \vdots \\ y_{i+(n/2)} \end{Bmatrix} \tag{B8}$$

That is, the coefficients for the nth-order high-pass filter are the negatives of the coefficients for the low-pass filter, except for the central coefficient $k = \frac{n}{2}$, which is equal to 2^n minus the central binomial coefficient $\binom{n}{n/2}$. Thus the sum of all the coefficients of the high-pass filter is zero. In the following arrays the left-hand set

represents the low-pass filters and the right-hand set the related high-pass filters. The normalizing factor for each set of coefficients is the sum of the binomial coefficients, 2^n.

n	2^n	Low Pass							High Pass						
2	4			1	2	1					-1	2	-1		
4	16		1	4	6	4	1			-1	-4	10	-4	-1	
6	64	1	6	15	20	15	6	1	-1	-6	-15	44	-15	-6	-1

The high-pass-filter characteristic $Z_n(f)$ for the nth-order filter is

$$Z_n(f) = 1 - Y_n(f)$$

$$= 1 - \cos^n \frac{\pi}{2} \frac{f}{f_F} \tag{B9}$$

which, for $n = 2$, is $\sin^2 \frac{\pi}{2} \frac{f}{f_F}$. The filter characteristic $Z_n(f)$ is plotted in figure 11(b) for comparison with $Y_n(f)$ (fig. 11(a)). As the order increases (and thus the length of time over which the filter "remembers" increases), the suppression of high-frequency components by the low-pass filter becomes more effective, and the filter becomes sharper; similarly, the pass band of the high-pass filter becomes wider.

Operations with low- and high-pass filters are commutative, and give band-pass filters. For example, combination of the second-order low-pass filter $\frac{1}{4}\lfloor 1 \quad 2 \quad 1 \rfloor$ and the high-pass operator $\lfloor -1 \quad 2 \quad -1 \rfloor$ is equivalent to the filter $\frac{1}{4}\lfloor -1 \quad 0 \quad 2 \quad 0 \quad -1 \rfloor$, which has a characteristic

$$F(f) = 4Y_2(f)Z_2(f)$$

$$= \sin^2 \frac{\pi f}{f_F} \tag{B10}$$

Similarly, the operator $\frac{1}{2}\lfloor -1 \quad 0 \quad 1 \rfloor$ (based on the first-order binomial coefficients) has a filter amplitude characteristic of

$$F(f) = \sin \frac{\pi f}{f_F} \tag{B11}$$

The band-pass filters can also be regarded as modified binomial filters for which the folding frequency has been redefined. For example, the operation $\frac{1}{4}\lfloor -1 \quad 0 \quad 2 \quad 0 \quad -1 \rfloor$ can be regarded as the high-pass filter of order 2 operating on the points y_{i-2}, y_i, and y_{i+2}; thus, in effect, the time interval Δt between data points is doubled, and the effective folding frequency is the value $\frac{f_F}{2} = \frac{1}{4\,\Delta t}$. Thus if $\frac{1}{4}\lfloor -1 \quad 2 \quad -1 \rfloor$ is represented by a filter factor

$$Z_2(f) = \sin^2 \frac{\pi}{2} \frac{f}{f_F}$$

the operator $\frac{1}{4}\lfloor -1 \quad 0 \quad 2 \quad 0 \quad -1 \rfloor$ represents the filter factor

$$F(f) = \sin^2 \frac{\pi}{2} \frac{f}{f_F/2} \tag{B12}$$

That is,

$$F(f) = \sin^2 \frac{\pi f}{f_F} \tag{B13}$$

which is the same as equation (B10).

Separation of Maneuvering and Buffet Loads

For the purposes of the present study a pair of low- and high-pass filters was developed. These filters, like the 28th-order binomial filters, operate on 29 successive values of the measured time history y_i, but differ from the binomial-type filters in both sharpness of discrimination at low frequencies and in suitability for routine computations with punched-card equipment. The filters are more easily described in terms of the low-pass member of the pair, which was constructed from the low-pass fourth-order binomial operator

$$\frac{1}{16}\lfloor 1 \quad 4 \quad 6 \quad 4 \quad 1 \rfloor \tag{B14a}$$

and the two related modified binomial operators with band-pass characteristics

$$\frac{1}{16}\lfloor 1 \quad 0 \quad 4 \quad 0 \quad 6 \quad 0 \quad 4 \quad 0 \quad 1 \rfloor \tag{B14b}$$

$$\frac{1}{16}\left[1 \quad 0 \quad 0 \quad 0 \quad 4 \quad 0 \quad 0 \quad 0 \quad 6 \quad 0 \quad 0 \quad 0 \quad 4 \quad 0 \quad 0 \quad 0 \quad 1\right] \qquad \text{(B14c)}$$

These operators, respectively, have the filter characteristics

$$Y_4(f) = \cos^4 \frac{\pi}{2} \frac{f}{f_F}$$

$$Y_4(2f) = \cos^4 \frac{\pi}{2} \frac{2f}{f_F}$$

$$Y_4(4f) = \cos^4 \frac{\pi}{2} \frac{4f}{f_F}$$

as shown in figure 12(a). The three operators (B14) can be used in succession with three passes of the simpler punched-card calculators, or with more elaborate equipment the filtering can be accomplished with the combined symmetrical operator which acts on 29 adjacent points:

$$\frac{1}{4096}\left[1 \; 4 \; 10 \; 20 \; 35 \; 56 \; 84 \; 120 \; 161 \; 204 \; 246 \; 284 \; 315 \; 336 \; 344 \; 336 \; . \; . \; . \; 1\right] \qquad \text{(B15)}$$

In either case, the filter factor $F(f)$ is given by the product of the filter factors of the three operators as

$$F(f) = \left(\cos \frac{\pi}{2} \frac{f}{f_F} \cos \frac{\pi}{2} \frac{2f}{f_F} \cos \frac{\pi}{2} \frac{4f}{f_F}\right)^4$$

which is illustrated in figure 12(b). As measured by the criterion of band width at the half-power point, $F(f) = 0.707$, this filter has a band width of $0.0575f_F$, or as used in the present studies, where $f_F = 50$ cps, the band width is 2.9 cps. It is thus sharper than the 28th-order binomial filter (fig. 12(a)) which operates on the same number of points. Four-tenths of one percent of the total transmission lies in three minor lobes located between the zeros at $\frac{f}{f_F} = 0.25$, 0.50, 0.75, and 1.00, and shown to an expanded scale in figure 12(b), but these lobes are all smaller than 0.0028 in amplitude.

In order to obtain the buffet load, the time-history values of the maneuver load obtained through use of the operator (B15) were substracted from the measured load time history. It could have been obtained directly

by use of the high-pass filter equivalent to the operator (B15) but, since the central coefficient of the filter would have then contained not three but four digits (4,096 - 344 = 3,752), the buffet load was obtained in two steps in order to preserve the computational efficiency associated with the three-digit coefficients of (B15).

REFERENCES

1. Anon.: Technical Report by the Accidents Investigation Sub-Committee on the Accident to the Aeroplane G-AAZK at Meopham, Kent, on 21st July, 1930. R. & M. No. 1360, British A.R.C., Jan. 1931.

2. Liepmann, H. W.: On the Application of Statistical Concepts to the Buffeting Problem. Jour. Aero. Sci., vol. 19, no. 12, Dec. 1952, pp. 793-800, 822. (Also available as "An Approach to the Buffeting Problem From Turbulence Considerations," Rep. No. SM-13940, Douglas Aircraft Co., Inc., Mar. 13, 1951.)

3. Huston, Wilber B., and Skopinski, T. H.: Measurement and Analysis of Wing and Tail Buffeting Loads on a Fighter Airplane. NACA Rep. 1219, 1955. (Supersedes NACA TN 3080, 1954.)

4. Rice, S. O.: Mathematical Analysis of Random Noise. Pts. I and II. Bell Syst. Tech. Jour., vol. XXIII, no. 3, July 1944, pp. 282-332; Pts. III and IV, vol. XXIV, no. 1, Jan. 1945, pp. 46-156.

5. Lawson, James L., and Uhlenbeck, George E., eds.: Threshold Signals. McGraw-Hill Book Co., Inc., 1950.

6. James, Hubert M., Nichols, Nathaniel B., and Phillips, Ralph S.: Theory of Servomechanisms. McGraw-Hill Book Co., Inc., 1947.

7. Press, Harry, and Houbolt, John C.: Some Applications of Generalized Harmonic Analysis to Gust Loads on Airplanes. Jour. Aero. Sci., vol. 22, no. 1, Jan. 1955, pp. 17-26, 60.

8. Anderson, R. L., and Bancroft, T. A.: Statistical Theory in Research. McGraw-Hill Book Co., Inc., 1952.

9. Fleck, John T., and Fryer, William D.: An Exploration of Numerical Filtering Techniques. Rep. No. XA-869-P-1, Cornell Aero. Lab., Inc., May 1, 1953.

TABLE I.- GROUND VIBRATION FREQUENCY OF AIRPLANE STRUCTURAL MODES

	Frequency, cps, for -	
	Basic airplane	Modified airplane
Wing modes:		
First symmetric bending	11.7	9.3
First asymmetric bending	22.3	18.1
First torsion	38.0	34.5
Second symmetric bending	-----	52.0
Horizontal stabilizer modes:		
First symmetric bending	25.0	25.0
First asymmetric bending	36.0	36.0
First torsion	70.0	70.0
Fuselage modes:		
Torsion	9.8	9.8
Side bending	12.5	12.5
Vertical bending	14.9	14.9

TABLE II.- FREQUENCY DISTRIBUTION OF LOADS AND LOAD PEAKS IN BUFFETING

Load range, lb	Frequency for -											
	Run A						Run B					
	Wing			Tail			Wing			Tail		
	Loads	Positive peaks	Negative peaks	Loads	Positive peaks	Negative peaks	Loads	Positive peaks	Negative peaks	Loads	Positive peaks	Negative peaks
-700 to -600	1		1				2		2			
-600 to -500	2		2	1		1	7		3	1		5
-500 to -400	11		8	0		0	8		4	7		3
-400 to -300	24	2	15	7		5	7		5	5		10
-300 to -200	30	2	16	20		7	17		8	20		16
-200 to -100	54	6	26	59		29	34	2	14	41	3	23
-100 to 0	73	14	20	116	9	25	79	8	21	80	5	10
0 to 100	84	22	13	105	28	9	86	20	7	90	29	4
100 to 200	47	19	1	49	20	2	34	14	2	47	19	1
200 to 300	30	14		25	15		19	10	3	15	9	
300 to 400	18	8		4	3		11	7	0	10	5	
400 to 500	7	6		3	2		9	4	1	0	0	
500 to 600	9	8		2	1		4	2		1	2	
600 to 700	1	1					2	2		3	1	
700 to 800							1	1				
N	391	102	102	391	78	78	320	70	70	320	73	73
Mean	1.4			0.8			6.5			1.9		
σ	219			142			220			173		
χ^2	10.1	16.2		7.5	7.40		56			15.6		
$\chi^2_{.05}$	14.1	19.7		11.1	7.82		14.1			11.1		

TABLE III.- FREQUENCY DISTRIBUTION OF TRANSFORMED LOADS AND LOAD PEAKS FOR RUN B

Range of L/P, lb	Frequency for -					
	Wing			Tail		
	Loads	Positive peaks	Negative peaks	Loads	Positive peaks	Negative peaks
-2,000 to -1,800	1		1			
-1,800 to -1,600	3		3			
-1,600 to -1,400	3		2			
-1,400 to -1,200	5		2	2		2
-1,200 to -1,000	10		6	4		4
-1,000 to -800	11		8	10		6
-800 to -600	21		8	22		15
-600 to -400	23		13	30	1	8
-400 to -200	38	2	7	42	4	16
-200 to 0	36	6	3	40	3	9
0 to 200	40	6	2	47	7	6
200 to 400	41	8	2	50	14	5
400 to 600	27	6	2	35	23	1
600 to 800	21	12		21	7	1
800 to 1,000	20	13		7	5	
1,000 to 1,200	10	6		6	5	
1,200 to 1,400	5	3		2	1	
1,400 to 1,600	3	3		1	1	
1,600 to 1,800	1	1		0	0	
1,800 to 2,000	0	0		1	1	
2,000 to 2,200	1	1				
N	320	67	67	320	73	72
Mean	25			25		
σ	653			512		
χ^2	19.8	4.7		4.8	5.5	
$\chi^2_{.05}$	22.4	11.1		14.1	11.1	

TABLE IV.- VALUES OF FREQUENCY PARAMETERS OBTAINED FROM POWER SPECTRA AND FROM TIME HISTORIES

Source	Wing			Tail		
	f_0, cps	f_p, cps	f_0/f_p	f_0, cps	f_p, cps	f_0/f_p
Run A:						
Spectrum	18.1	34.8	0.52	15.5	25.4	0.61
Time history	16.3	26.2	.62	15.7	20.0	.78
Run B:						
Spectrum	16.4	27.3	.60	15.5	28.1	.55
Time history	14.8	21.8	.68	16.1	22.8	.70
Run B (transformed):						
Time history	14.8	21.0	.77	16.1	22.7	.71

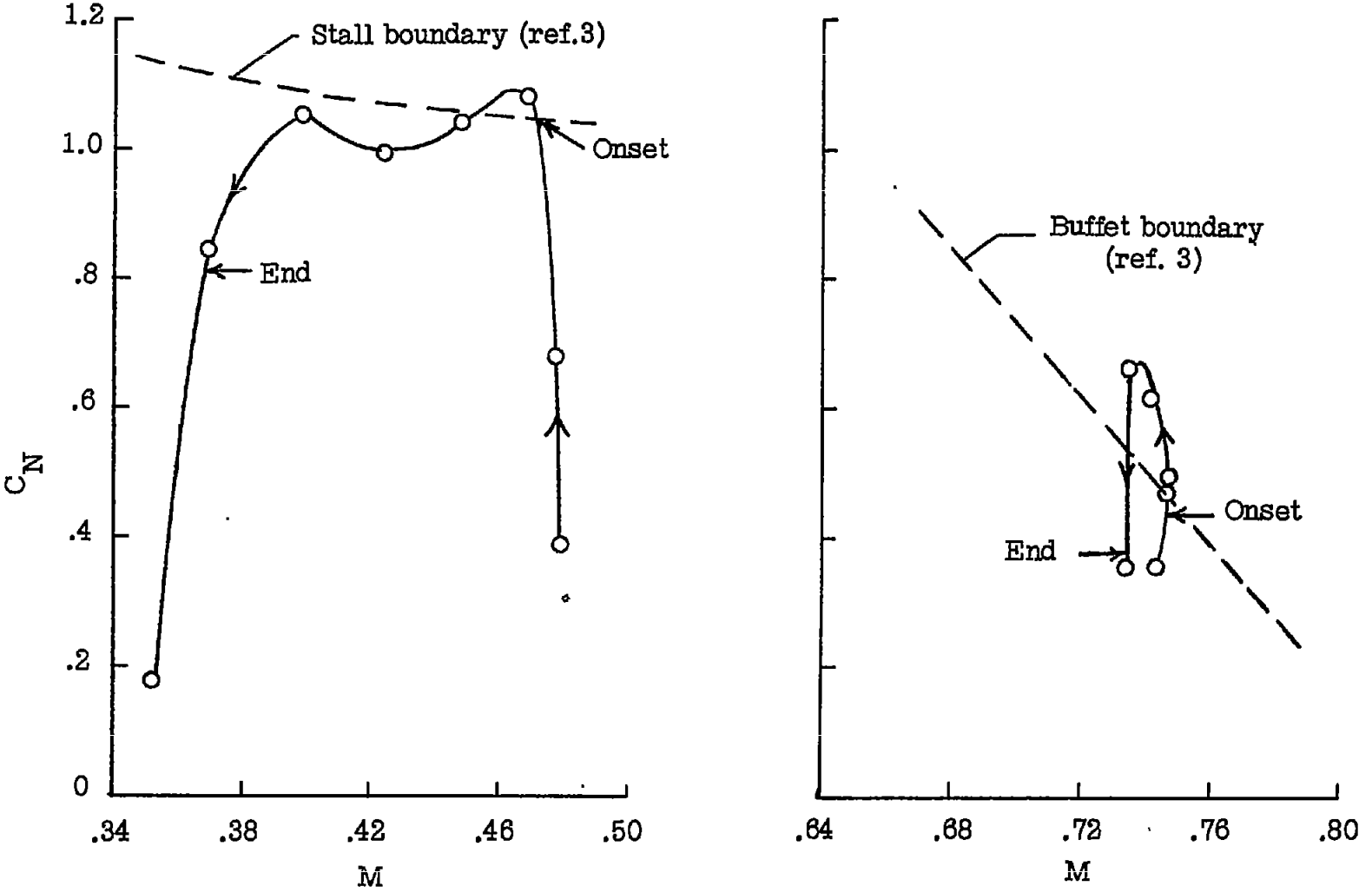

(a) Run A.

(b) Run B.

Figure 1.- Maneuvers analyzed in present investigation.

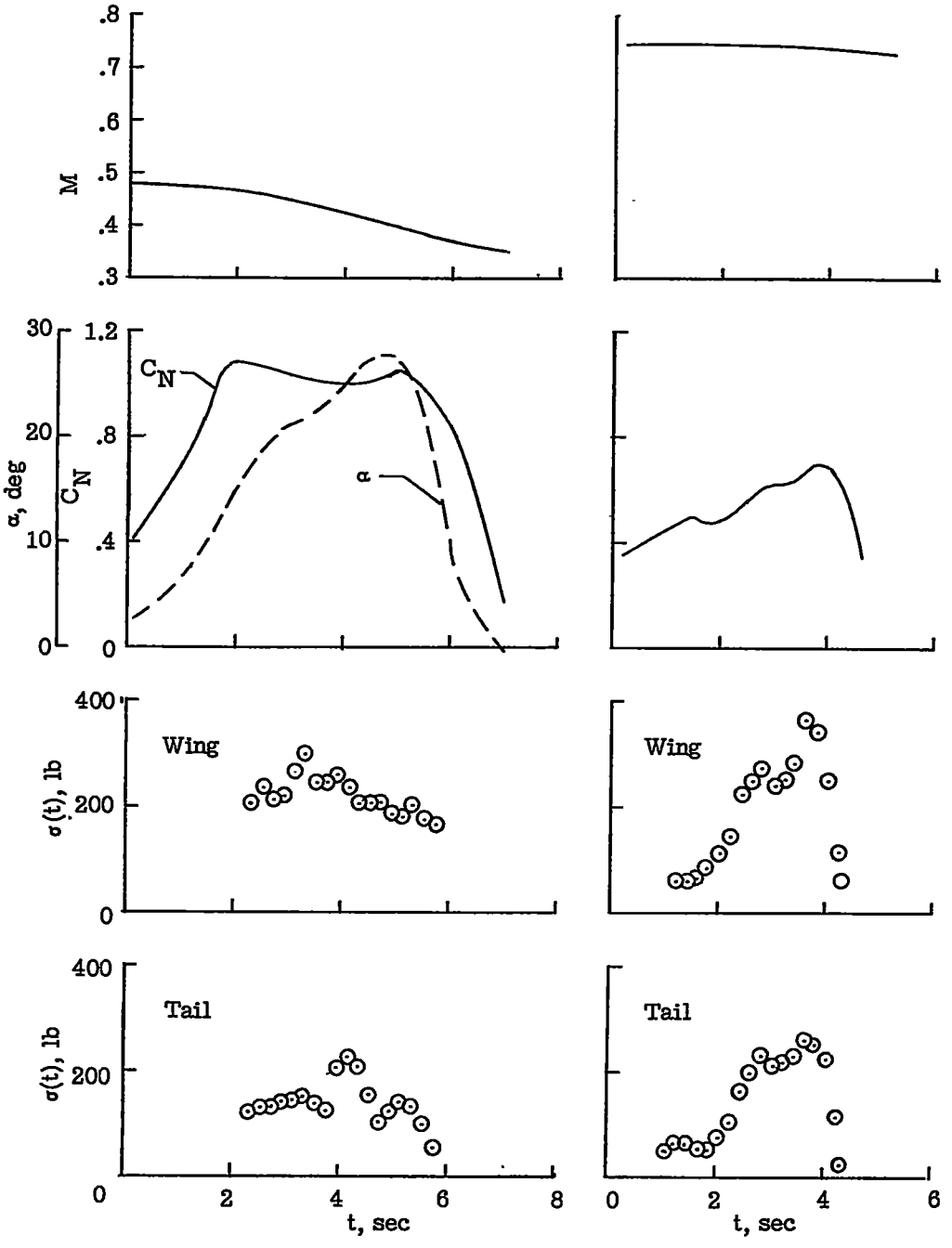

(a) Run A; M ≈ 0.46.

(b) Run B; M ≈ 0.74.

Figure 2.- Time variation of airplane operating conditions and buffet intensity.

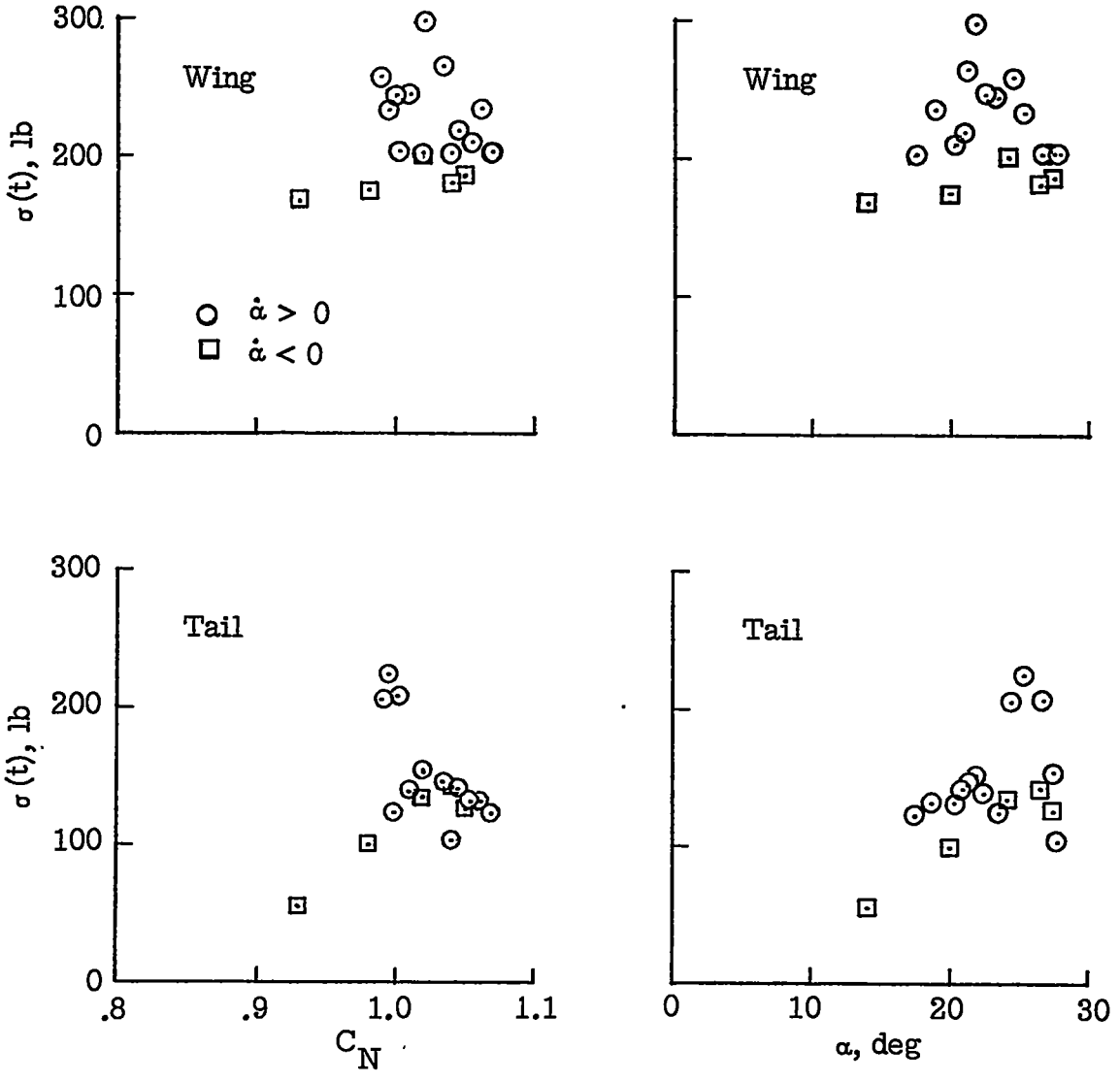

(a) Variation with C_N. (b) Variation with α.

Figure 3.- Variation of wing and tail buffet load with C_N and α in stall. Run A.

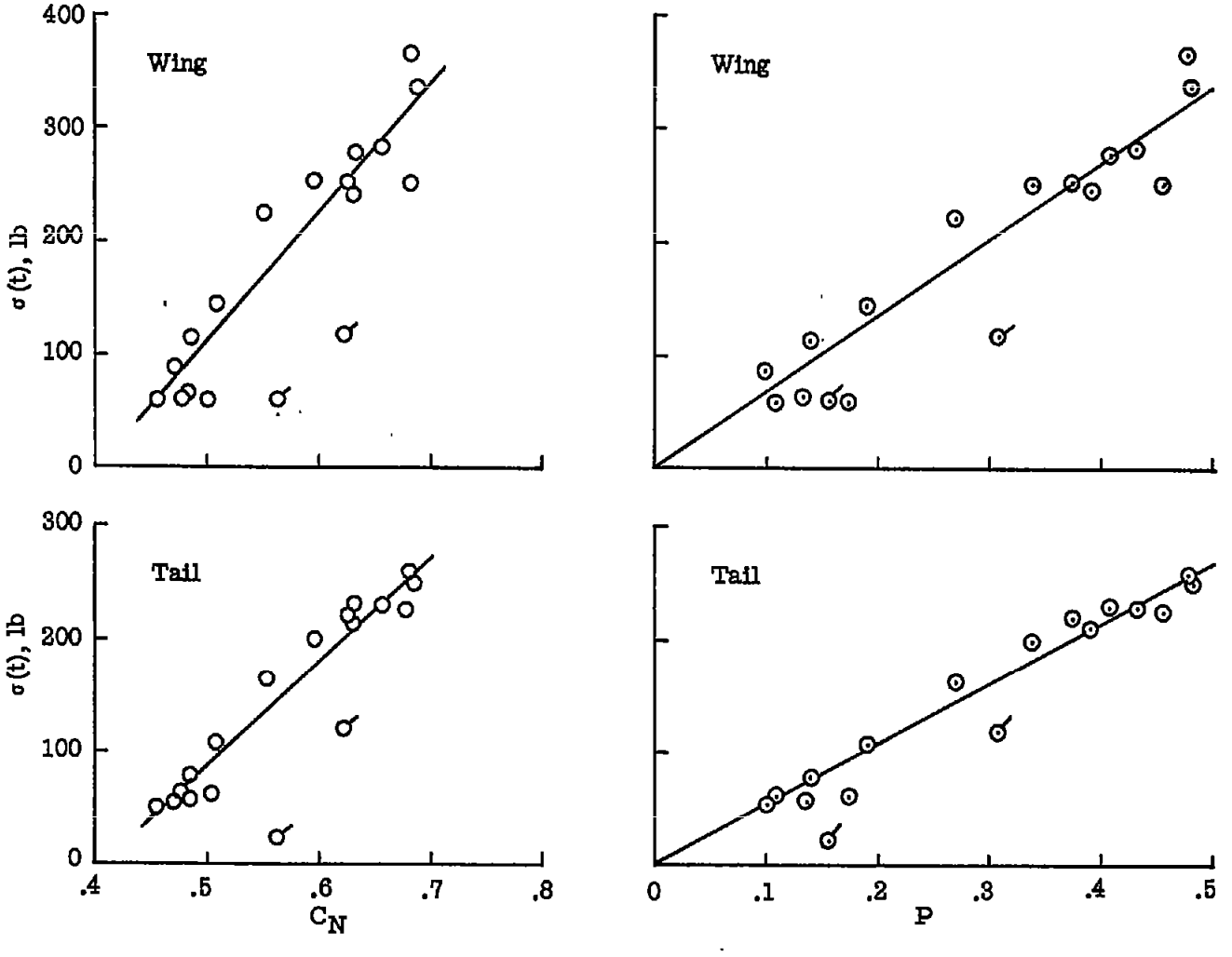

(a) Variation with C_N.

(b) Variation with penetration P.

Figure 4.- Variation of wing and tail buffet load with C_N and P in shock regime. Run B.

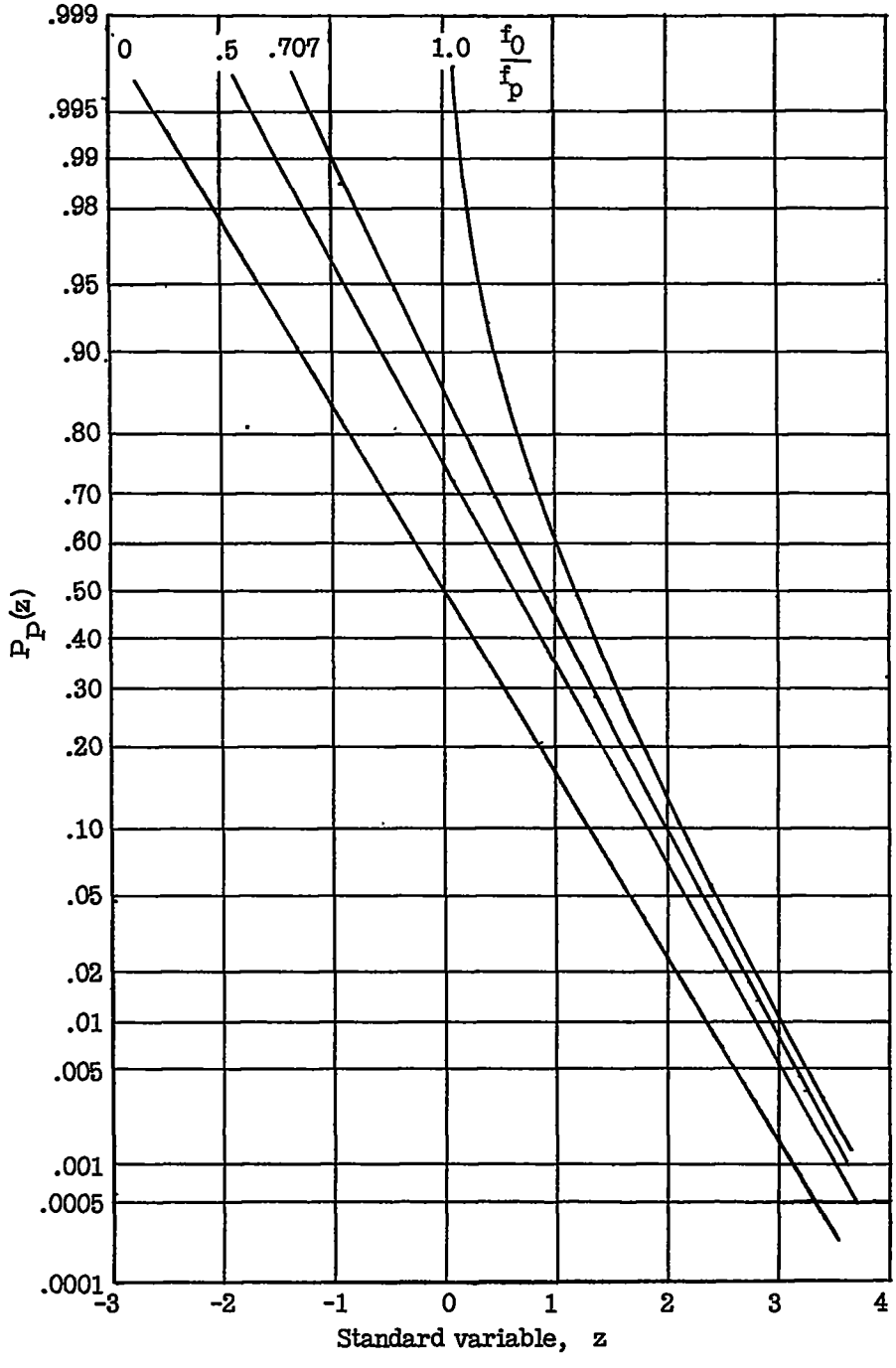

(a) Probability $P_p(z)$ that a peak will exceed a given value.

Figure 5.- Peak probability functions of a Gaussian random process for various values of the ratio f_0/f_p.

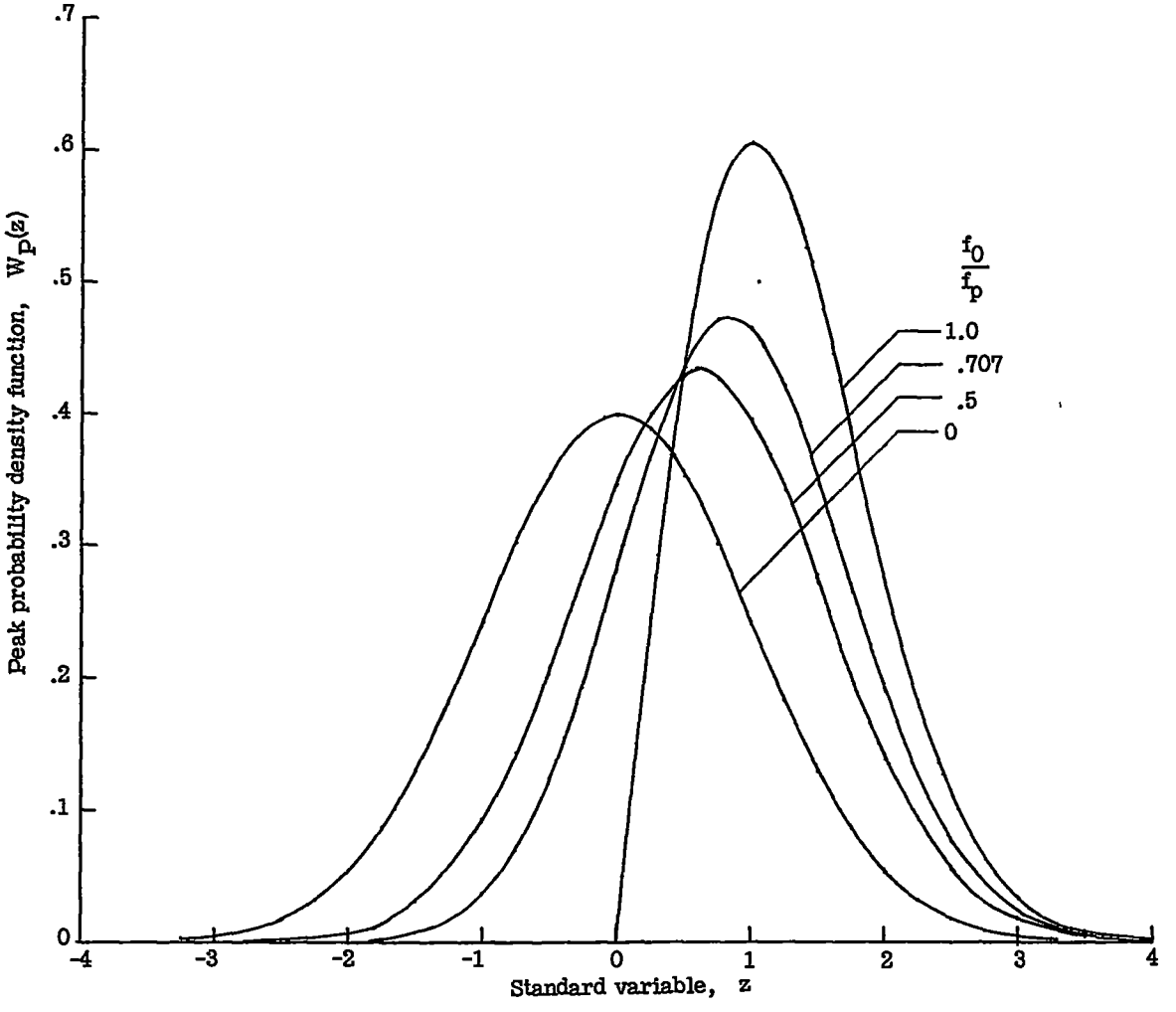

(b) Peak probability density $W_p(z)$.

Figure 5.- Concluded.

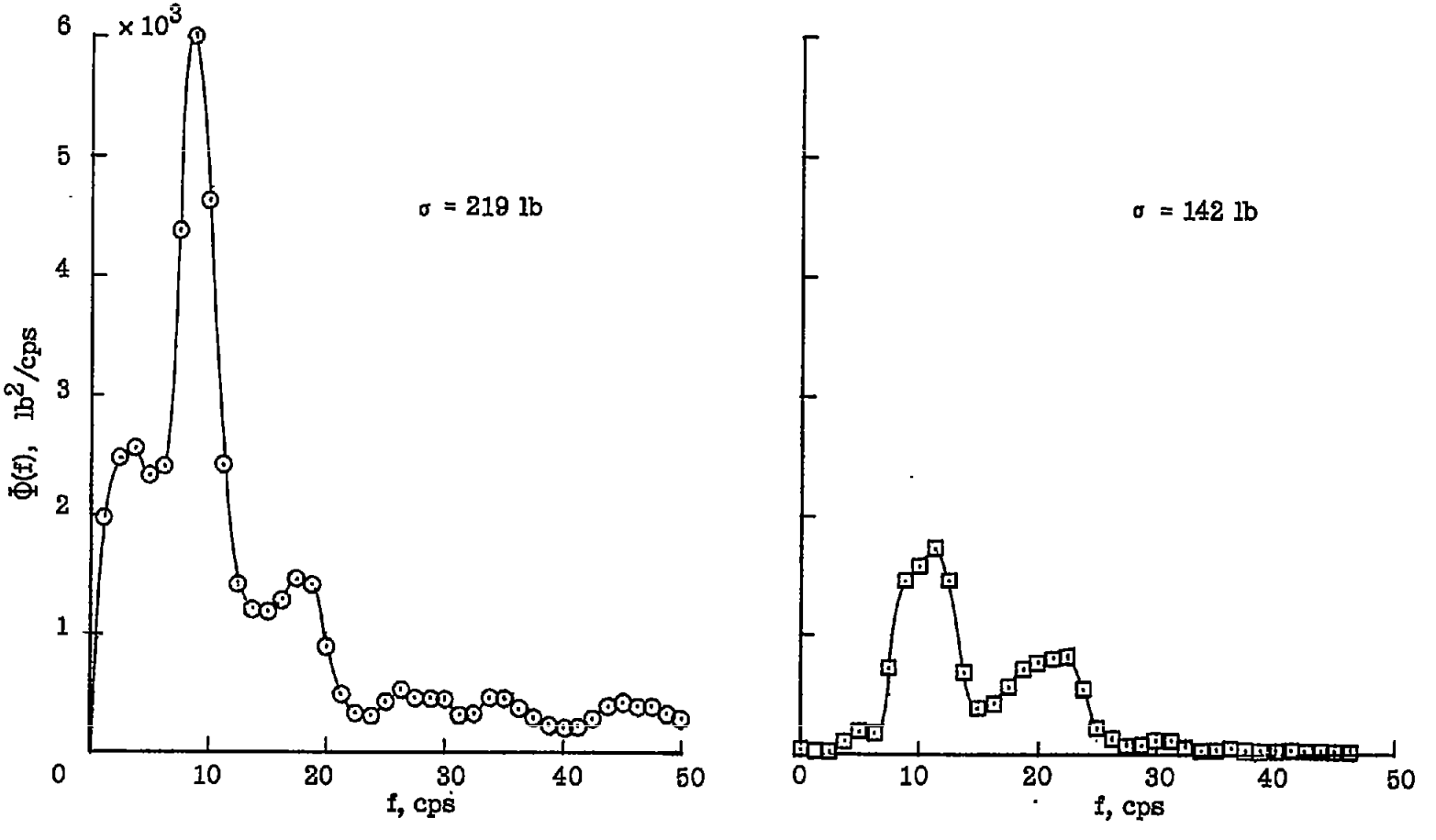

(a) Run A; wing load.

(b) Run A; tail load.

Figure 6.- Power spectrum of buffet load.

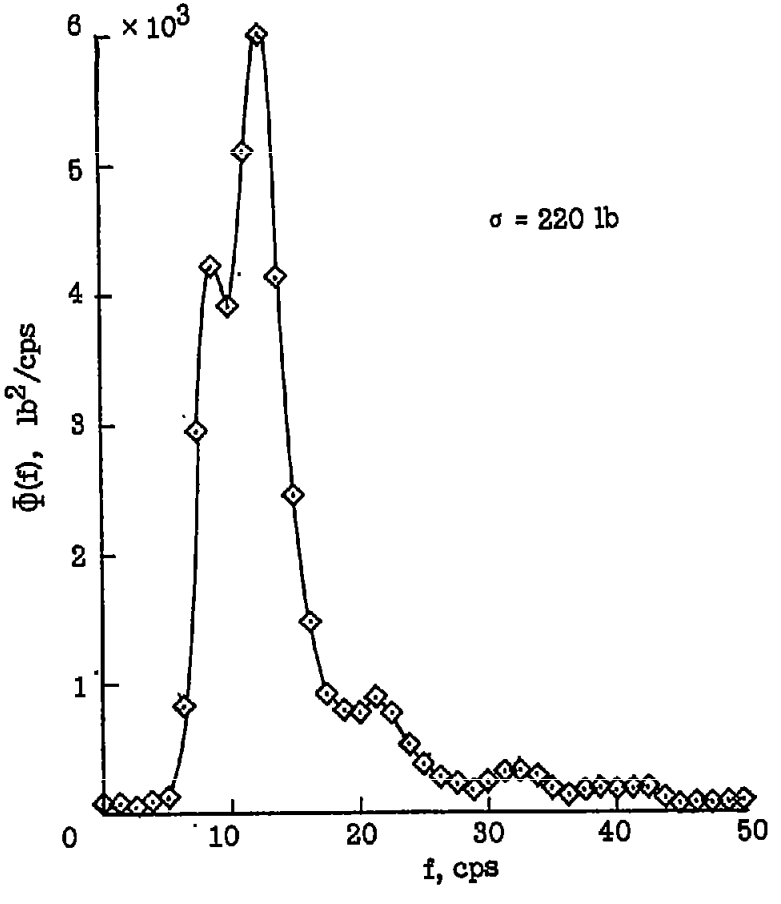

(c) Run B; wing load.

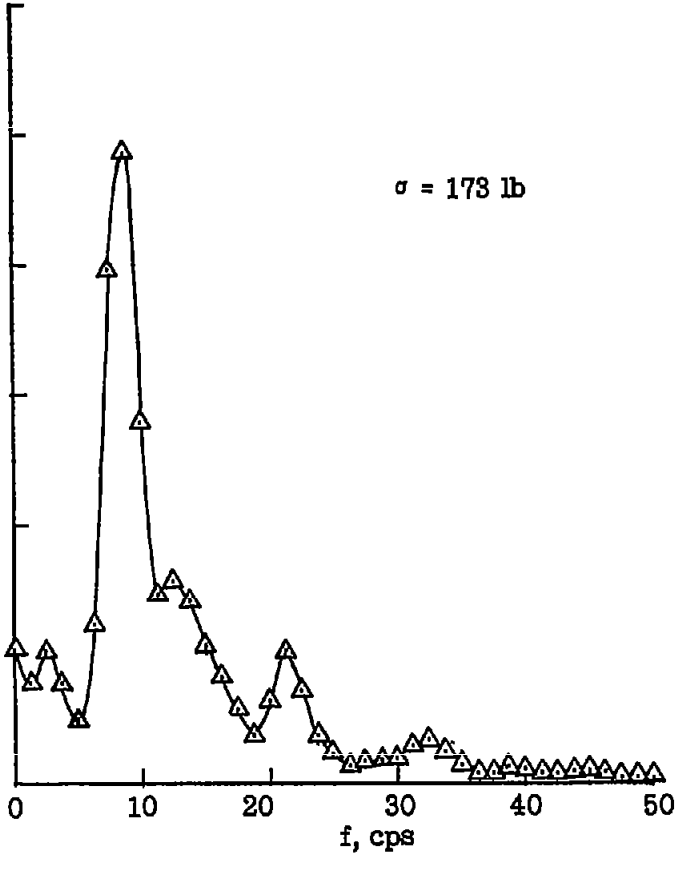

(d) Run B; tail load.

Figure 6.- Concluded.

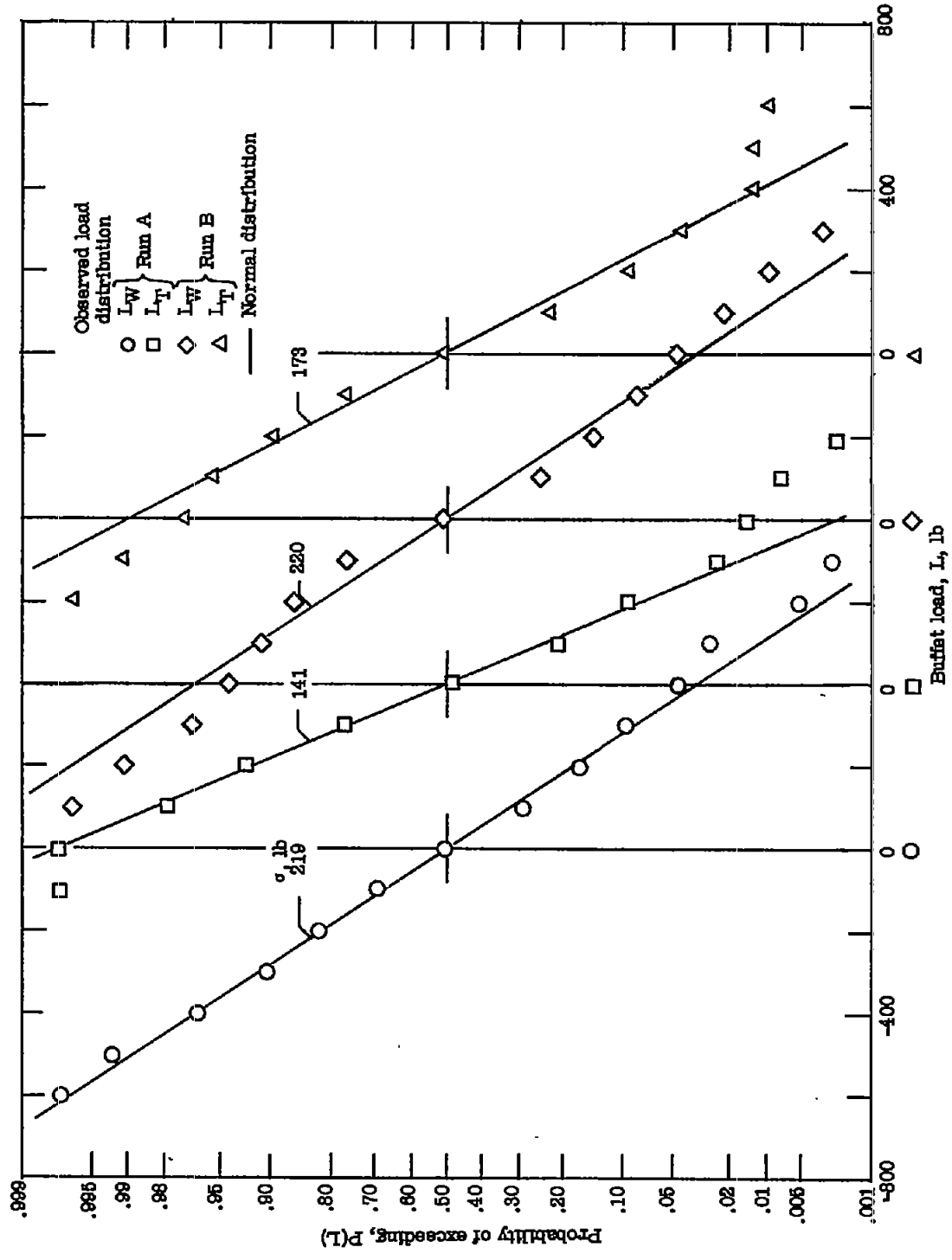

Figure 7.- Probability that a value of buffet load L will be exceeded.

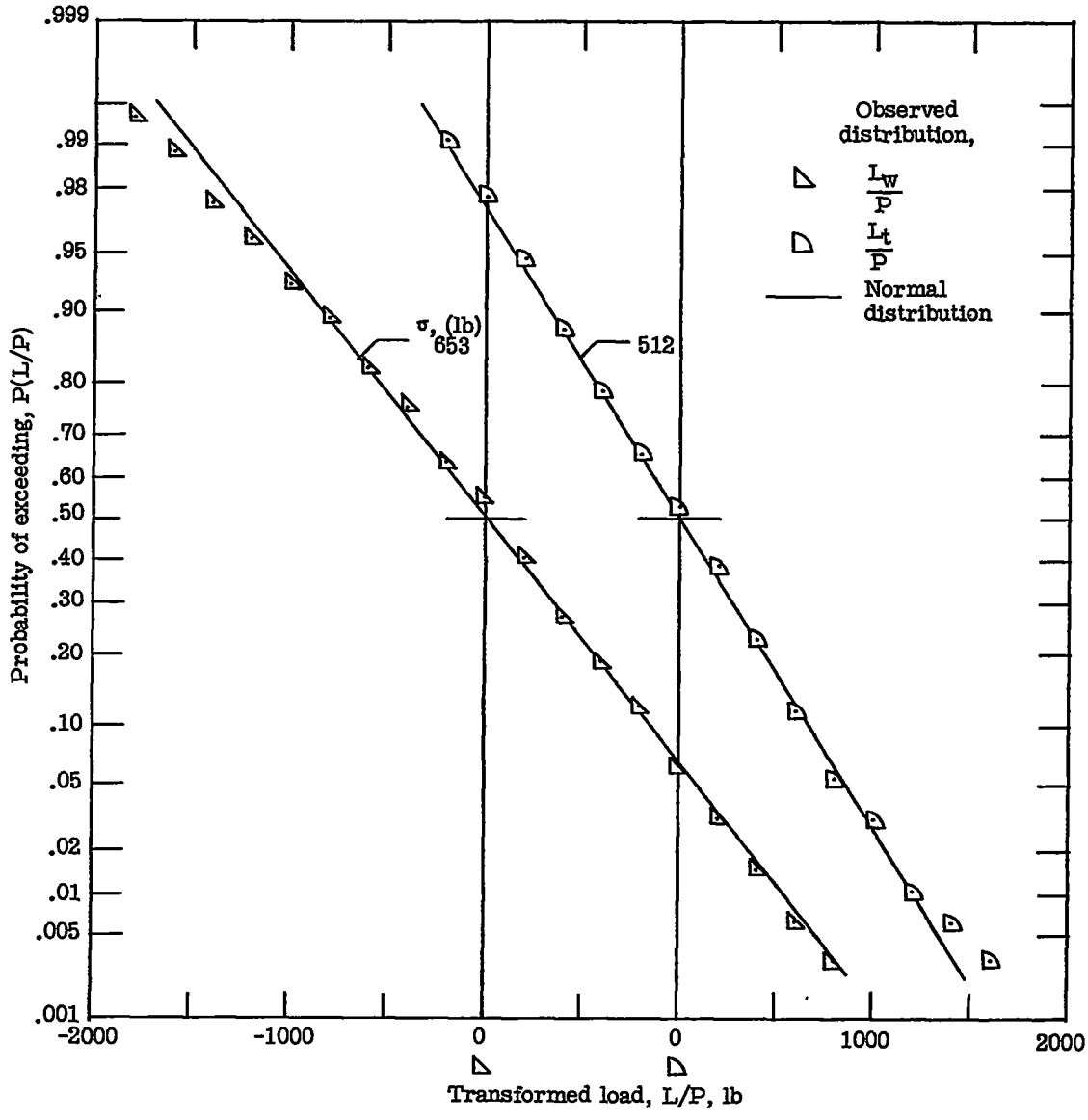

Figure 8.- Probability that a value of transformed load L/P will be exceeded.

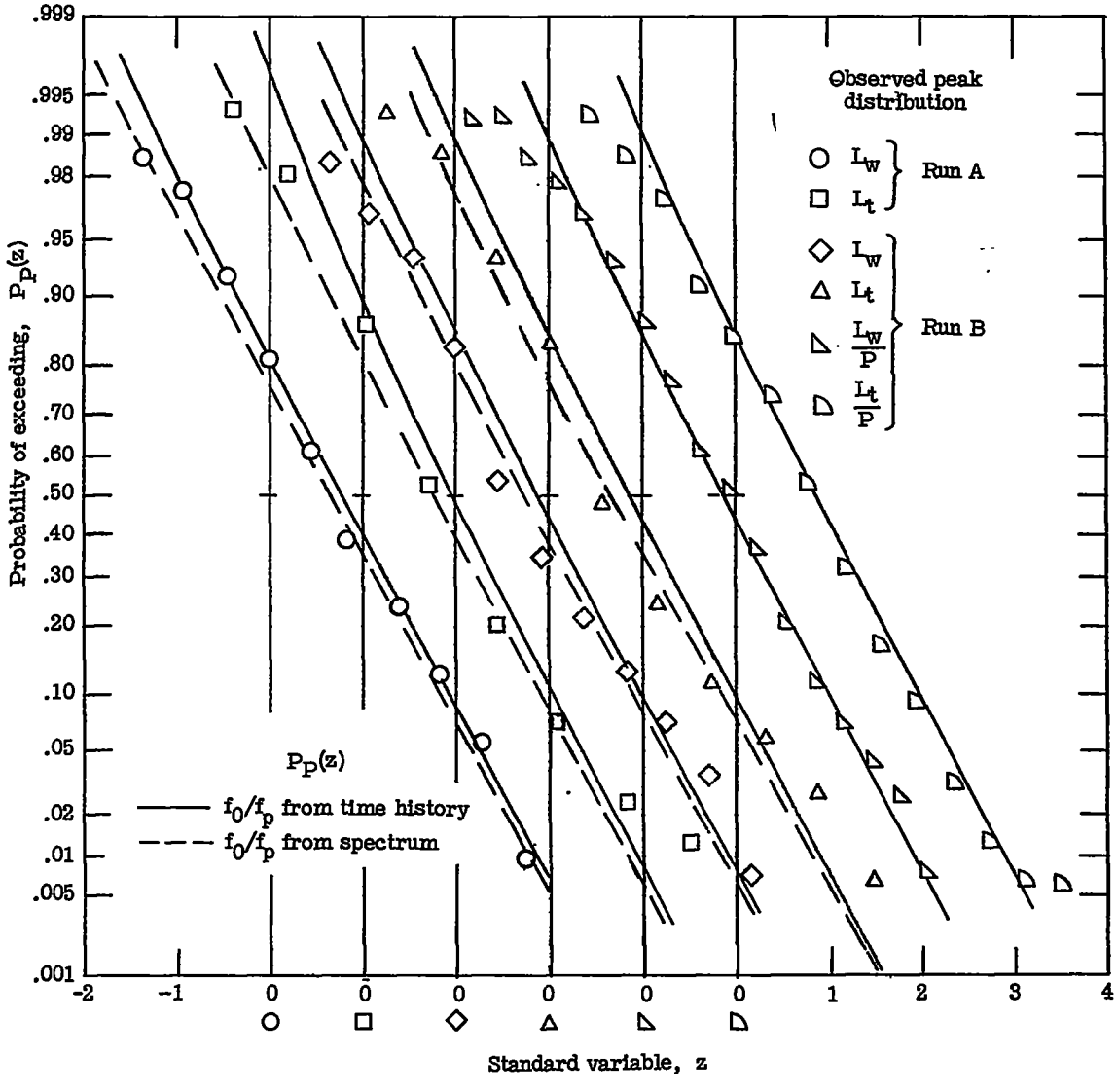

Figure 9.- Probability that a peak value of buffet load will exceed a value equal to $z\sigma$.

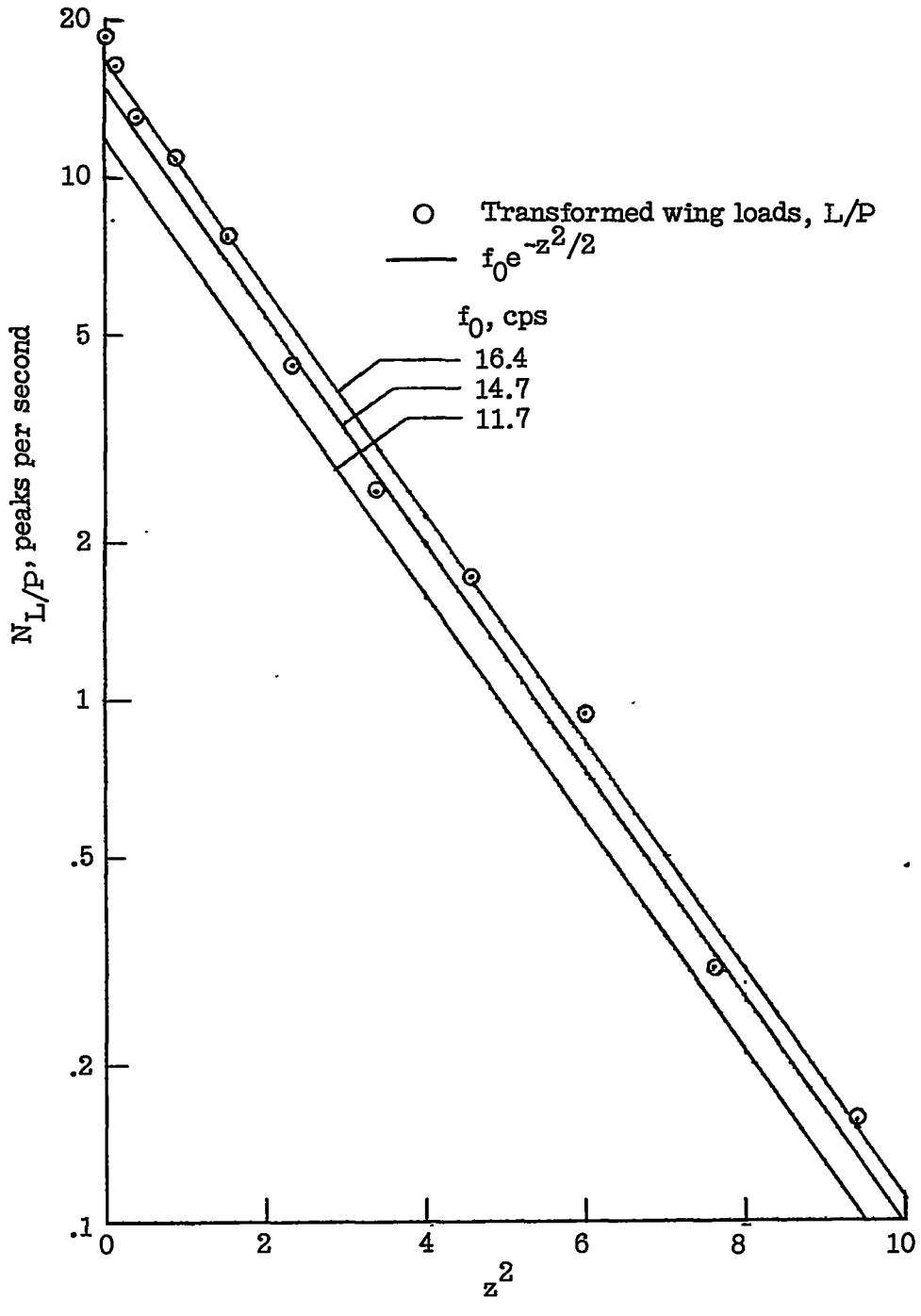

Figure 10.- Observed number of peaks per second of run B which exceed a value of L/P, compared with Rice's asymptotic expression for peak frequency.

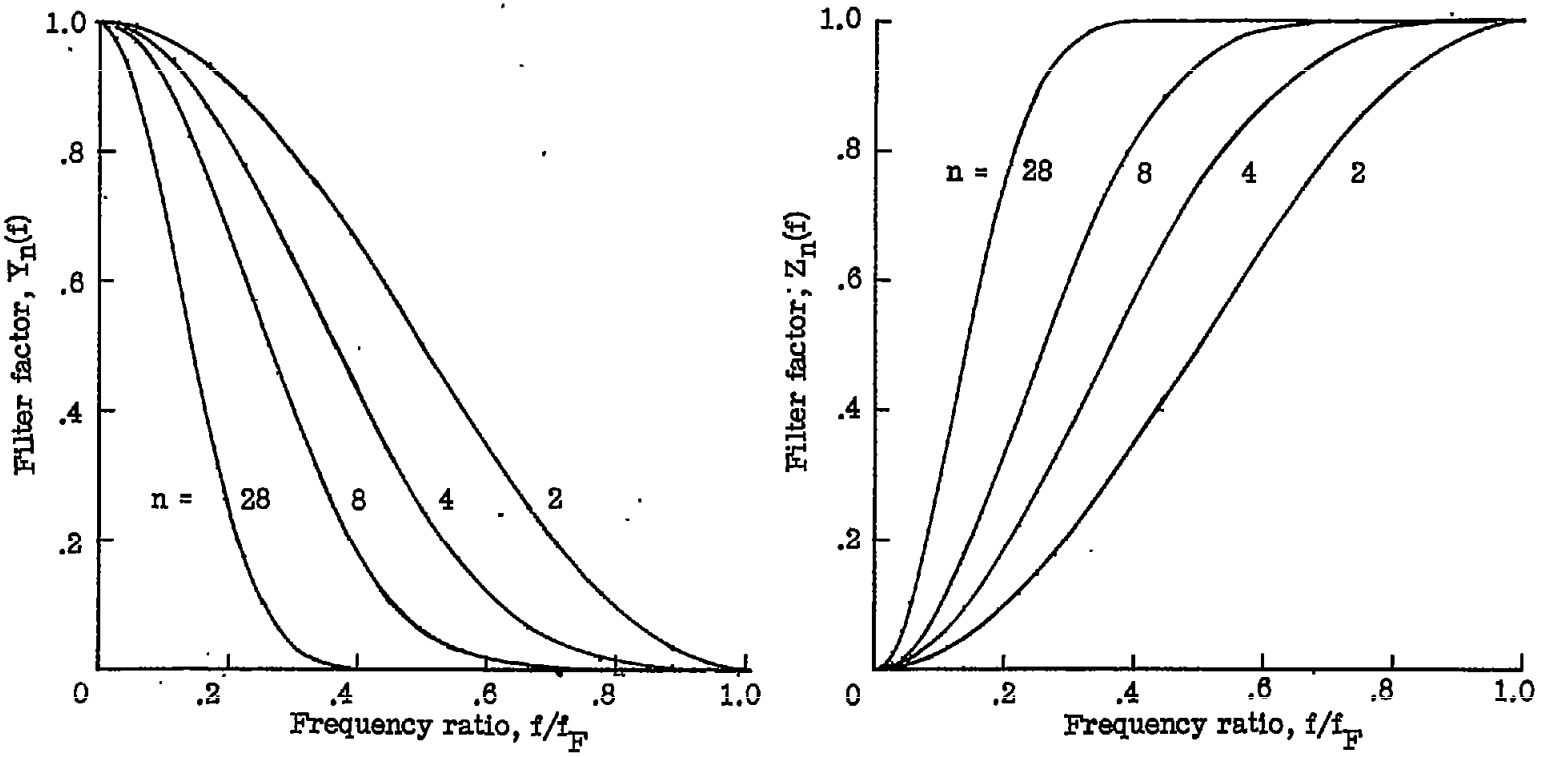

(a) Low-pass filter.

(b) High-pass filter.

Figure 11.- Filter factor of binomial filter of order n and associated high-pass filter.

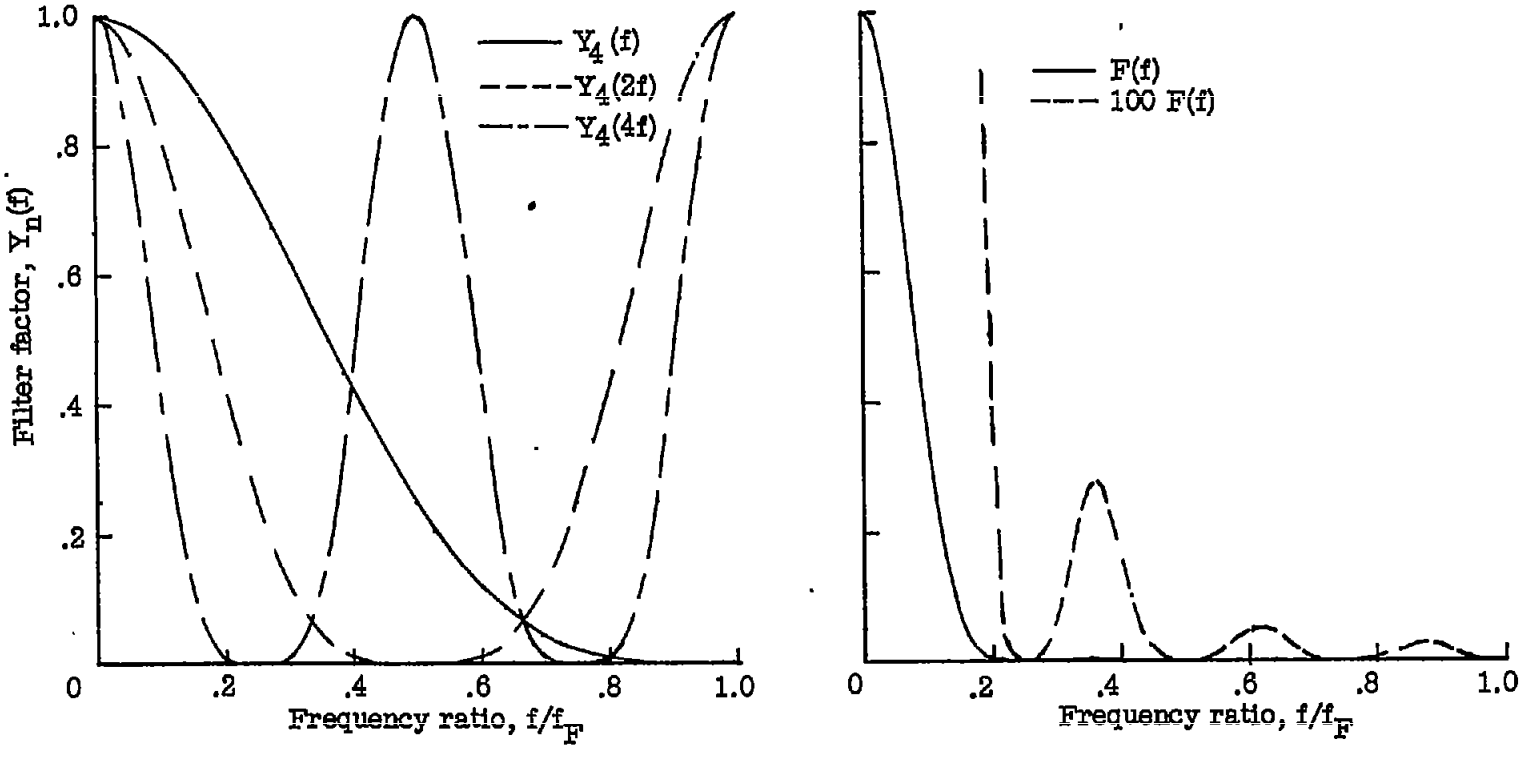

(a) Elementary filters.

(b) Low-pass filter used.

Figure 12.- Construction of the numerical filter for separating total load measurements into maneuvering and buffet components.